EUROPEAN JOURNAL OF PURE AND APPLIED MATHEMATICS
2026, Vol. 19, Issue 2, Article Number 7182
ISSN 1307-5543 – ejpam.com
Published by New York Business Global

Analysis of Lumpy Skin Disease Transmission via Optimal Control and Numerical Verification by Neural Network

Aman Ullah[1], M. A. El-Shorbagy[2,*], Mumtaz Ali Shah[1], Mati ur Rahman[3], Hossam A. Nabwey[2], M. M. Nour[2]

[1] *Department of Mathematics, University of Malakand, Dir(L), Khyber Pakhtunkhwa, Pakistan*
[2] *Department of Mathematics, College of Science and Humanities in Al-Kharj, Prince Sattam bin Abdulaziz University, Al-Kharj 11942, Saudi Arabia*
[3] *Department of Mathematics and Statistics, College of Sciences, Imam Mohammad Ibn Saud Islamic University (IMSIU), Riyadh, Saudi Arabia*

Abstract. Lumpy skin disease (LSD) mainly targets cattle, particularly buffalo and cows and it is characterised by the development of lumps or nodules on the skin and other parts throughout the body. This disease leads to significant losses in dairy production and cattle populations, making it crucial to address this issue through a mathematical modelling approach. In this work, we formulate a mathematical model to understand the spread of LSD considering all potential routes through which the disease may propagate within a community. We investigate basic results in the model and determine its equilibrium points. The model undergoes sensitivity analysis as well as local stability and global stability analysis assuming the basic reproductive number is less than one. We explore the uniqueness, existence, boundedness and feasibility of the model's solutions. To prevent the spread of the disease and we introduce a new vaccination class into the model and the model is extended to include optimal control to a mathematical model strategies focusing on vaccination and treatment to evaluate their effectiveness to minimize infection and costs. The results demonstrate that a combination of targeted vaccination and timely treatment can significantly reduce the spread of LSD supporting the implementation of cost-effective control measures. This modelling approach provides valuable insights for policymakers and veterinary health authorities in designing effective disease management strategies. The model is then solved by using Euler's method and the results are graphically displayed using MATLAB. An Artificial Neural Network (ANN) is also employed to approximate solution and analyze system dynamics. This approach provides effective strategies and accurate predictions for managing complex processes.

2020 Mathematics Subject Classifications: 92D30, 34D20, 49J15, 37N25

Key Words and Phrases: Lumpy skin disease, equilibrium points, sensitivity analysis, local and global stability analysis, basic reproductive number, optimal control theory, neural network.

*Corresponding Author.
DOI: https://doi.org/10.29020/nybg.ejpam.v19i2.7182

Email addresses: ma.hassan@psau.edu.sa (M. A. El-Shorbagy)

1. Introduction

Lumpy Skin Disease (LSD) is a viral disease that mainly affects cattle. Main symptoms of LSD are fever, depression, skin lesions, and swelling in different areas of the body such as legs, nose and eyes [1]. Additional signs include reduced milk production, swollen legs and difficulty walking [2]. The most susceptible population are lactating cows and young calves that are exposed to the disease [3]. In Africa and the Middle East, LSD is declared as an endemic, recently reported in Turkey and Pakistan. The disease also impacted Greece in 2015 and 2016 and subsequently spread to Bulgaria and North Macedonia [4]. The economic consequences of LSD are considerable, resulting losses in production such as decreased milk yields, lower quality of skin, as well as imposing trade and transport restrictions in affected regions [5]. Lumpy Skin Disease is mainly spread through insect vectors, including mosquitoes, flies and ticks or through the use of contaminated needles [6]. Such a type of vector can spread the virus by travelling in vehicles or being carried by wind from regions where the disease is endemic. The specific insect species responsible for transmission may vary by country, though this aspect has not been extensively studied [7]. LSD tends to spread most rapidly in warm, humid conditions, particularly during the summer and fall when insect activity, especially that of flies its peak [8]. Additionally, water, contaminated feed, and equipment can contribute to the transmission of the virus. Notably, LSD is not transmissible to humans [9]. To prevent the spread of insects such as mosquitoes and flies between locations, it is recommended that vehicles not be brought near areas where animals reside unless they are thoroughly have been properly disinfected with products deemed safe for animal environments. In addition to minimise the risk of infection it is advisable to use insect repellents that are safe for animals or relocate them to areas with fewer biting flies. Ensuring that different needles are used when treating animals is also crucial. Other general preventive measures include disinfecting the one entrance to stables, requiring visitors to wear disposable boot covers, suits, cleaning and disinfecting vehicles before in after use. Further, precautions involve avoiding contact between animals from different herds such as on shared pastures and refraining from grazing in areas with high fly populations. Additionally, sharing animals equipment, trucks or personnel between farms should be avoided [10]. Lumpy Skin Disease has recently affected livestock in Pakistan, particularly in the Sindh province, resulting in the death of over 36000 cows in 2022. The disease has spread to the Punjab province exacerbating the crisis in the country's livestock sector. Small-scale farmers, particularly those with fewer than 50 animals are experiencing significant financial strain. With the approaching Eidal-Adha, the demand for healthy animals has surged, causing prices to skyrocket beyond the reach of many individuals, leading to substantial economic losses for farmers and potentially driving them into poverty [11]. The Punjab livestock department has expressed concern over its lack of funds to purchase vaccines leaving farmers to bear the high costs themselves with a 100 ml bottle of vaccine Live Attenuated Vaccines (LAVs) priced at Rs. 44000 an amount many farmers cannot afford. Cases of LSD have also been reported in some regions of Khyber Pukhtunkhwa with animals having been similarly affected. Given these challenges both the government and the livestock department must intervene and support

farmers who are unable to vaccinate their animals [12]. Without timely intervention the livelihoods of many small farmers are at risk [13].
Mathematical models are now a vital approach for analysing the dynamics and behaviour of infectious diseases spreading, including those affecting livestock and could be instrumental in offering insights and recommendations for controlling LSD outbreaks [14]. Lumpy Skin Disease (LSD) continues to pose a significant threat to cattle populations and agricultural economies, particularly in regions with limited access to veterinary infrastructure [15]. While vaccination and treatment are recognised as effective control strategies, implementing these interventions, optimally balancing cost and effectiveness is essential [16].
In this section, we extend the deterministic *SIVR* model of LSD by incorporating time-dependent control variables that represent vaccination $u_1(t)$ and treatment $u_2(t)$ strategies. The goal is to reduce the number of susceptible and infected cattle while minimizing the associated costs of intervention [16]. By applying Pontryagins Maximum Principle, we derive the necessary conditions for optimal control and formulate a cost functional that reflects the trade off between disease burden and resource expenditure [17]. This approach not only provides a theoretical framework for understanding how different control strategies influence disease dynamics but also offers practical insights for policymakers and veterinary health planners [18]. The numerical simulations of the optimal control problem demonstrate how well-designed strategies can significantly reduce the spread of LSDV, especially when resources are limited [19]. Artificial intelligence (AI), specially artificial neural networks (ANNs), has highly advanced the analysis and there arrangement of epidemic spread [20]. Alfwzan et al., developed the LSD using the modified parameterized approach as given below [21]. In future research the proposed model can be extended to a fractal fractional order derivative framework to incorporate memory and hereditary effects inherent in the system [22]. Solving the model using fractal fractional order derivatives may provide a more accurate and realistic representation of the dynamics compared to the integer order approach [23]. Further, studies can focus on the developing efficient numerical schemes for this extended model and analyzing its stability control strategies and sensitivity to various parameters [24]. Kenneth Levenberg and Donald Marqurdt developed the Levenberg Marquardt (LM) alogrithm a widely used method for efficiently training artificial neural networks by minimizing nonlinear squares errors [25, 26].

2. Materials and Techniques

We must consider that the *SIVR* model is a deterministic model as it is more suitable for high population sizes. The *SIVR* model is a type of model that divides the population into distinct groups or compartments hence the overall population is categorised into different classes. There are three types of cattle population insects population and contaminated environment [20]. This model accurately captures the rapidly increasing spread of the lumpy skin disease.

2.1. Model Assumption

To model an infectious disease by a mathematically certain assumptions must be according on the based in characteristics of the disease under investigation, in the case of lumpy skin disease. *SIVR* model for lumpy skin disease as this study is based in the following set of assumption:

(i) The recruitment rate of newborn and incoming animals is assumed to enter the population as susceptible.

(ii) It is assumed that all cattle in the population are vulnerable to contracting the lumpy skin disease.

(iii) All individuals have an equal chance of being infection can occur through contact with infected individuals, excluding those who are already immune to LSD.

(iv) Individuals who transmit the infection are quickly identified and isolated for prompt medical care and awareness.

(v) Population is assumed to be uniformly mixed, which means that the population consistently interacts with each other.

(vi) In the size of population changes, where the rate of entry and exit are not constant during each time step.

(vii) Recovered individuals from the disease gain lifelong immunity they cannot be re-infected again.

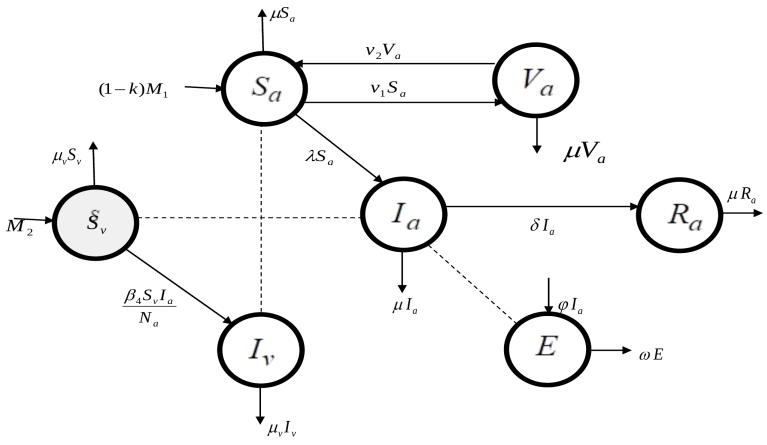

Figure 1: Flow-chart of the model LSD

Compartments	Descriptions
$\mathscr{N}_a(t)$	Total population of the cattle
$\mathscr{S}_a(t)$	The size of susceptible population
$\mathscr{I}_a(t)$	Infected cattle
$\mathscr{R}_a(t)$	The total of recovered cattle from the disease
$\mathscr{N}_v(t)$	The complete insects population
$\mathscr{S}_v(t)$	In the susceptible insect present at a time t
$\mathscr{I}_v(t)$	The infected insect
$\mathscr{E}(t)$	Contaminated environment

Table 1: Description of the compartments used in the model at a specific time, t

The LSD is a contagious viral illness and it's impact on cattle and leads to swellings legs, lameness, color discharges, nasal and cases swellings over the mucous membranes, along with the skin inflammation with raised nodules in the skin. In mathematically analysis for the study of this disease we represent the total cattle population by $\mathscr{N}_a$ in any time and further classify it into the susceptible compartment in the cattle $\mathscr{S}_a(t)$, infected compartment in the cattle is denoted by $\mathscr{I}_a(t)$, vaccinated compartment in the cattle is shown by $\mathscr{V}_a(t)$ and recovered compartment in the cattle is represented by $\mathscr{R}_a(t)$. So that

$$\mathscr{N}_a(t) = \mathscr{S}_a(t) + \mathscr{I}_a(t) + \mathscr{V}_a(t) + \mathscr{R}_a(t).$$

In transmission of this infection into the overall population of these things insect vectors like mosquitoes, flies and ticks play a role for spreading the infection so the population of insect is represented by $\mathscr{N}_v(t)$ and further categorized into insects that are susceptible is represented by $\mathscr{S}_v(t)$ and infected insects is denoted by $\mathscr{I}_v(t)$, so

$$\mathscr{N}_v(t) = \mathscr{S}_v(t) + \mathscr{I}_v(t).$$

The unclean environment is indicted as $\mathscr{E}(t)$, with certain viruses could be travel through air currents or within moving vehicles from a areas where the infection exists. Moreover the illness can spread through consumption of tainted water, feed, instruments and injections. It is also confirmed that in summer and autumn season the spread is most likely to be increased highly because flies are most prevalent. In the model (1), the development of uninfected cattle population is denoted by $(1-k)M_1$ whereas in the rate in which cattle naturally die is denoted by μ. Rate at which uninfected cattle come into effective contact in the transmission is denoted by λ, in the β_a is a ratio of insects rate of contact and all population of the cattle, β_b is ratio of contact rate due to environment transmission and total population of the cattle, β_c is ratio of contact rate it refers to the disease is passed on through direct contact from infected cattle into other healthy cattle and the total cattle population. Since in the virus remains in the sperm of infected bulls it can spread through mating or insemination. It has been observed that infected female cattle during pregnancy deliver to calves in the time of birth skin lesions. Nursing calves can become infected through sores present on the teats or by consuming milk that contains the virus. The rate at which infected cattle recover is symbolized by δ. Parameter M_2

Parameters	Descriptions
$(1-k)M_1$	Population growth rate of healthy cattle
μ	Natural death rate among the cattle
λ	Effective contact rate for the disease transmission in which the healthy cattle catched the infection
β_a	The ratio of contact rate of insects and all cattle population
β_b	Ratio of contact rate due to environment transmission and total population of cattle
β_c	Ratio of contact rate is directly transmission of infection from sick cattle to healthy cattle and the total cattle population
δ	The recovery rate of infected cattle
M_2	Growth rate of insects (vector) population
μ_v	Normal death rate in insects(vector)
β_4	The interaction among the susceptible insects and infected cattle
ϕ	Virus left the environment of infected insects
ω	Virus disinfection rate
v_1	The rate of vaccine in which we give to susceptible cattle
v_2	The rate of loss of immunity

Table 2: Description of the parameters used in the model

represents insects growth rate while μ_v is represented the natural death rate. Rate of contact in the susceptible insects and infected cattle is denoted by β_4. In parameter ϕ denote amount of virus left the environment of infected cattle, it also be acknowledged that vehicles and individuals associated with the stable can contaminate in environment. The disinfection of virus is denoted by ω. To illustrates the parameters and its description of the model (1) is given in Table 2.

$$\begin{cases} \frac{d\mathscr{S}_a(t)}{dt} &= (1-k)M_1 - \beta_a\mathscr{S}_a\mathscr{I}_v - \beta_b\mathscr{S}_a\mathscr{E} - \beta_c\mathscr{S}_a\mathscr{I}_a - \mu\mathscr{S}_a - v_1\mathscr{S}_a + v_2\mathscr{V}_a \\ \frac{d\mathscr{I}_a(t)}{dt} &= \beta_a\mathscr{S}_a\mathscr{I}_v + \beta_b\mathscr{S}_a\mathscr{E} + \beta_c\mathscr{S}_a\mathscr{I}_a - (\delta+\mu)\mathscr{I}_a \\ \frac{d\mathscr{V}_a(t)}{dt} &= kM_1 + v_1\mathscr{S}_a - v_2\mathscr{V}_a - \mu\mathscr{V}_a \\ \frac{d\mathscr{R}_a(t)}{dt} &= \delta\mathscr{I}_a - \mu\mathscr{R}_a \\ \frac{d\mathscr{S}_v(t)}{dt} &= M_2 - \frac{\beta_4\mathscr{S}_v\mathscr{I}_a}{\mathscr{N}_a} - \mu_v\mathscr{S}_v \\ \frac{d\mathscr{I}_v(t)}{dt} &= \frac{\beta_4\mathscr{S}_v I_a}{\mathscr{N}_a} - \mu_v\mathscr{I}_v \\ \frac{d\mathscr{E}(t)}{dt} &= \phi\mathscr{I}_a - \omega\mathscr{E}, \end{cases} \tag{1}$$

where $\lambda(t) = \beta_a\mathscr{I}_v + \beta_b\mathscr{E} + \beta_c\mathscr{I}_a$, and the initial conditions are as follows:

$$\mathscr{S}_a(0) > 0, \mathscr{I}_a(0) \geq 0, \mathscr{V}_a(0) > 0, \mathscr{R}_a(0) \geq 0, \mathscr{S}_v(0) \geq 0, \mathscr{I}_v(0) \geq 0, \mathscr{E}(0) \geq 0. \tag{2}$$

2.2. Characteristics of the Model

In the fundamental features in the model of *SIVR* include feasibility and positivity of the solution. The acceptable solution in the equations of the model defines in a region in which the solution of equation in biologically meaningful while Positivity of the solution ensures the outcomes remain non negative of the solution in model equation.

2.2.1. Uniqueness and Existence

Existence and uniqueness of solutions ensure that the disease dynamics described by the model are biologically realistic and deterministic, meaning that for given initial conditions, the system will evolve in a predictable way without ambiguity.

2.2.2. Boundedness

Boundedness implies that population sizes of cattle and insects remain within realistic biological limits, ensuring that no population grows unbounded or becomes negative.

2.2.3. Feasible Solution

An the *SIVR* model is applied in to the infectious disease within a cattle population to be assuming all used in the parameters in all compartments at initial conditions are non negative.

The set of feasible solution which represent the positive fixed region on the model is defined as follows:

$$\begin{aligned}
\mathscr{W} &= \left\{(\mathscr{S}_a, \mathscr{I}_a, \mathscr{V}_a, \mathscr{R}_a) \in R_+^4 : \mathscr{N}_a(t) = \mathscr{S}_a(t) + \mathscr{I}_a(t) + \mathscr{V}_a(t) + \mathscr{R}_a(t) \to \frac{(1-k)M_1}{\mu}\right\}.\\
\mathscr{W}' &= \left\{(\mathscr{S}_v, \mathscr{I}_v) \in R_+^2 : \mathscr{N}_v(t) = \mathscr{S}_v(t) + \mathscr{I}_v(t) \to \frac{M_2}{\mu_v}\right\}.
\end{aligned}$$

This claim is supported the following Lemmas.

Lemma 1. *In set $\mathscr{W}$ is positively fixed and draws each solution within R_+^4.*

Proof. Hence $\mathscr{N}_a(t) = \mathscr{S}_a(t) + \mathscr{I}(t) + \mathscr{V}_a(t) + \mathscr{R}_a(t)$. Taking derivative w. r. t. t we get

$$\frac{d\mathscr{N}_a}{dt} = \frac{d\mathscr{S}_a}{dt} + \frac{d\mathscr{I}_a}{dt} + \frac{d\mathscr{V}_a}{dt} + \frac{d\mathscr{R}_a}{dt}. \tag{3}$$

Putting all the values of model (1) in equation (3) to get the total cattle population rate is change over time, i.e.,

$$\begin{aligned}
\frac{d\mathscr{N}_a}{dt} &= (1-k)M_1 - \mu\mathscr{S}_a - \mu\mathscr{I}_a - \mu\mathscr{V}_a - \mu\mathscr{R}_a\\
\frac{d\mathscr{N}_a}{dt} &= (1-k)M_1 - \mu(\mathscr{S}_a + \mathscr{I}_a + \mathscr{V}_a + \mathscr{R}_a),
\end{aligned}$$

which gives $\frac{d\mathscr{N}_a}{dt} = (1-k)M_1 - \mu\mathscr{N}_a$, after simplification we get

$$\mathscr{N}_a(t) = \frac{(1-k)M_1}{\mu} + ke^{(-\mu t)}, \tag{4}$$

putting $t = 0$ we get

$$\begin{aligned}\mathscr{N}_a(0) &= \frac{(1-k)M_1}{\mu} + k \\ \Rightarrow k &= \mathscr{N}_a(0) - \frac{(1-k)M_1}{\mu}.\end{aligned}$$

Putting in the values in k the simplified solution of this linear differential equation will becomes in the following expression:

$$\mathscr{N}_a(t) = \mathscr{N}_a(0)e^{-\mu t} + \frac{(1-k)M_1}{\mu}\left(1 - e^{(-\mu t)}\right). \tag{5}$$

Taking limit as $t \to \infty$ we have $\mathscr{N}_a(t) \leq \frac{(1-k)M_1}{\mu}$. Hence, it has been confirmed that $\mathscr{W}$ remains positively invariant and attracts every solutions within the region R_+^4.

Lemma 2. *Within set of $\mathscr{W}$ is positively invariant and draws every solution within R_+^2.*

Proof. We know that $\mathscr{N}_v(t) = \mathscr{S}_v(t) + \mathscr{I}_v(t)$,

$$\frac{d\mathscr{S}_v}{dt} = M_2 - \frac{\beta_4\mathscr{S}_v\mathscr{I}_a}{\mathscr{N}_a} - \mu_v\mathscr{S}_v, \tag{6}$$

$$\frac{d\mathscr{I}_v}{dt} = \frac{\beta_4\mathscr{S}_v\mathscr{I}_a}{\mathscr{N}_a} - \mu_v\mathscr{I}_v, \tag{7}$$

Adding Equations (6) and (7) to get rate of change over time on the insect population i.e.,

$$\begin{aligned}\frac{d\mathscr{N}_v}{dt} &= \frac{d\mathscr{S}_v}{dt} + \frac{d\mathscr{I}_v}{dt} \\ \frac{d\mathscr{N}_v}{dt} &= M_2 - \mu_v\mathscr{S}_v - \mu_v\mathscr{I}_v \\ \frac{d\mathscr{N}_v}{dt} &= M_2 - \mu_v(\mathscr{S}_v + \mathscr{I}_v) \\ \frac{d\mathscr{N}_v}{dt} &= M_2 - \mu_v\mathscr{N}_v,\end{aligned}$$

it is a first order linear differential equation. First order linear differential equation in the from of:

$$M_2 = \frac{d\mathscr{N}_v}{dt} + \mu_v\mathscr{N}_v. \tag{8}$$

After simplification we get:

$$\mathscr{N}_v(t) = \mathscr{N}_v(0)e^{-\mu_v t} + \frac{M_2}{\mu_v}\left(1 - e^{-\mu_v t}\right). \tag{9}$$

Taking limit as $t \to \infty$ we have $\mathscr{N}_v(t) \leq \frac{M_2}{\mu_v}$. Therefore it has been conformed that $\mathscr{W}$ is positively invariant and satisfies each solution within R_+^2.

$$\Omega = \left\{ \mathscr{W} \in R_+^4 : \mathscr{N}_a(t) \leq \frac{(1-k)M_1}{\mu}, \mathscr{W}' \in R_+^2 : \mathscr{N}_v(t) \leq \frac{M_2}{\mu_v}, \mathscr{E} \in R_+ : \frac{(1-k)M_1\phi}{\mu\omega} \right\},$$

where $\mathscr{W} = (\mathscr{S}_a(t), \mathscr{I}_a(t), \mathscr{V}_a(t), \mathscr{R}_a(t))$ and $\mathscr{W}' = (\mathscr{S}_v(t), \mathscr{I}_v(t))$.

2.2.4. Results of Positivity

The next step we will prove that all variables in model *SIVR* all the equation $\frac{d\mathscr{S}_a}{dt}, \ldots, \frac{d\mathscr{R}_a}{dt}$ it will be non-negative.

Lemma 3. *Let the starting set of data is to be given be* $(\mathscr{S}_a, \mathscr{I}_a, \mathscr{V}_a, \mathscr{R}_a)(0) \in \mathscr{W}$, *the solution set* $(\mathscr{S}_a, \mathscr{I}_a, \mathscr{V}_a, \mathscr{R}_a, \mathscr{S}_v, \mathscr{I}_v, \mathscr{E})$ *of the equations* $\frac{d\mathscr{S}_a}{dt}, \frac{d\mathscr{I}_a}{dt}, \frac{d\mathscr{V}_a}{dt}, \frac{d\mathscr{R}_a}{dt}, \frac{d\mathscr{S}_v}{dt}, \frac{d\mathscr{I}_v}{dt}, \frac{d\mathscr{E}}{dt}$ *are positive for every* $t > 0$.

Proof. In model (1) consider that

$$\frac{d\mathscr{S}_a}{dt} = (1-k)M_1 - \beta_a\mathscr{S}_aI_v - \beta_b\mathscr{S}_aI_a - \mu\mathscr{S}_a - v_1\mathscr{S}_a + v_2\mathscr{V}_a \geq -\left(\beta_a\mathscr{S}_aI_v + \beta_b\mathscr{S}_a\mathscr{I}_a - \mu\mathscr{S}_a - v_1\mathscr{S}_a\right), \tag{10}$$

that is

$$\begin{aligned} \frac{d\mathscr{S}_a}{dt} &\geq -\left(\beta_a\mathscr{I}_v + \beta_b\mathscr{I}_a + \mu + v_1\right)\mathscr{S}_a \\ \frac{d\mathscr{S}_a}{\mathscr{S}_a} &\geq -\left(\beta_a\mathscr{I}_v + \beta_b\mathscr{I}_a + \mu + v_1\right)dt \text{ since } \mathscr{S}_a \neq 0 \end{aligned}$$

By performing integrating on both sides of the inequalities, we have :

$$\begin{aligned} \ln\left(\mathscr{S}_a(t)\right) &\geq -\left(\beta_a\mathscr{I}_v + \beta_b\mathscr{I}_a + \mu + v_1\right)t + k \\ \mathscr{S}_a(t) &\geq ke^{(-(\beta_aI_v + \beta_bI_a + \mu + v_1)t)}. \end{aligned}$$

At $t = 0$, it turns into

$$\mathscr{S}_a(t) \geq \mathscr{S}_a(0)e^{(-(\beta_aI_v + \beta_bI_a + \mu + v_1)(0))} \geq 0.$$

Hence, $(\beta_a\mathscr{I}_v + \beta_b\mathscr{I}_a + \mu + v_1) \geq 0$, that means

$$\mathscr{S}_a(t) > 0. \tag{11}$$

By the same way, it can be straightforwardly concluded that all the remaining of equations of model (1) are all positive.

2.3. Existence and Uniqueness of the Solution

In general ODE of the first-order is given as follows:

$$x' = f(t,x), x(t_0) = x_0. \tag{12}$$

To answers the following questions:

(i) In which conditions lead to the existence of a solution for the equation (12)?

(ii) In which cases can we ensure that the solution of the equation is unique (12)?

Consider

$$\frac{d\mathscr{U}}{dt} = \mathscr{F}(t,u(t));\ u(0) = u_0 \tag{13}$$

$$\mathscr{U} = (\mathscr{S}_a, \mathscr{I}_a, \mathscr{V}_a, \mathscr{R}_a, \mathscr{S}_v, \mathscr{I}_v, \mathscr{E}) \tag{14}$$

$$\mathscr{U}_0 = (\mathscr{S}_a(0), \mathscr{I}(0), \mathscr{V}_a(0), \mathscr{R}_a(0), \mathscr{S}_v(0), \mathscr{I}_v(0), \mathscr{E}(0)) \tag{15}$$

$$\frac{d\left(\mathscr{S}_a, \mathscr{I}_a, \mathscr{V}_a, , \mathscr{R}_a, \mathscr{S}_v, \mathscr{I}_v, \mathscr{E}\right)}{dt} = \mathscr{F}\left(t, (\mathscr{S}_a, \mathscr{I}_a, \mathscr{V}_a, \mathscr{R}_a, \mathscr{S}_v, \mathscr{I}_v, \mathscr{E})\right) \tag{16}$$

$$\frac{d\mathscr{U}}{dt} = \mathscr{F}(t,u(t)), u(0) = u_0 \tag{17}$$

$$\begin{cases} \mathscr{U} = (\mathscr{S}_a, \mathscr{I}_a, \mathscr{V}_a, \mathscr{R}_a, \mathscr{S}_v, \mathscr{I}_v, \mathscr{E}) \\ \mathscr{U}_0 = (\mathscr{S}_a(0), \mathscr{I}(0), \mathscr{V}_a(0), \mathscr{R}_a(0), \mathscr{S}_v(0), \mathscr{I}_v(0), \mathscr{E}(0)) \\ \frac{d(\mathscr{S}_a, \mathscr{I}_a, \mathscr{V}_a, , \mathscr{R}_a, \mathscr{S}_v, \mathscr{I}_v, \mathscr{E})}{dt} = \mathscr{F}(t, (\mathscr{S}_a, \mathscr{I}_a, \mathscr{V}_a, \mathscr{R}_a, \mathscr{S}_v, \mathscr{I}_v, \mathscr{E})). \end{cases} \tag{18}$$

We get

$$\begin{cases} f_1\left(t, \mathscr{S}_{an}, \mathscr{I}_{an}, \mathscr{V}_{an}, \mathscr{R}_{an}, \mathscr{S}_{vn}, \mathscr{I}_{vn}, \mathscr{E}_n\right) & = \frac{d\mathscr{S}_a}{dt} \\ f_2\left(t, \mathscr{S}_{an}, \mathscr{I}_{an}, \mathscr{V}_{an}, \mathscr{R}_{an}, \mathscr{S}_{vn}, \mathscr{I}_{vn}, \mathscr{E}_n\right) & = \frac{d\mathscr{I}_a}{dt} \\ f_3\left(t, \mathscr{S}_{an}, \mathscr{I}_{an}, \mathscr{V}_{an}, \mathscr{R}_{an}, \mathscr{S}_{vn}, \mathscr{I}_{vn}, \mathscr{E}_n\right) & = \frac{d\mathscr{V}_a}{dt} \\ f_4\left(t, \mathscr{S}_{an}, \mathscr{I}_{an}, \mathscr{V}_{an}, \mathscr{R}_{an}, \mathscr{S}_{vn}, \mathscr{I}_{vn}, \mathscr{E}_n\right) & = \frac{d\mathscr{R}_a}{dt} \\ f_5\left(t, \mathscr{S}_{an}, \mathscr{I}_{an}, \mathscr{V}_{an}, \mathscr{R}_{an}, \mathscr{S}_{vn}, \mathscr{I}_{vn}, \mathscr{E}_n\right) & = \frac{d\mathscr{S}_v}{dt} \\ f_6\left(t, \mathscr{S}_{an}, \mathscr{I}_{an}, \mathscr{V}_{an}, \mathscr{R}_{an}, \mathscr{S}_{vn}, \mathscr{I}_{vn}, \mathscr{E}_n\right) & = \frac{d\mathscr{I}_v}{dt} \\ f_7\left(t, \mathscr{S}_{an}, \mathscr{I}_{an}, \mathscr{V}_{an}, \mathscr{R}_{an}, \mathscr{S}_{vn}, \mathscr{I}_{vn}, \mathscr{E}_n\right) & = \frac{d\mathscr{E}}{dt} \end{cases} \tag{19}$$

$$\mathscr{U}(t) = \mathscr{U}_0 + \int_0^t \mathscr{F}\left(t, \mathscr{U}(t)dt\right). \tag{20}$$

$$\begin{aligned} &(\mathscr{S}_a(t), \mathscr{I}_a(t), \mathscr{V}_a(t), \mathscr{R}_a(t), \mathscr{S}_v(t), \mathscr{I}_v(t), \mathscr{E}(t)) \\ &= (\mathscr{S}_{a,0}, \mathscr{I}_{a,0}, \mathscr{V}_{a,0}, \mathscr{R}_{a,0}, \mathscr{S}_{v,0}, \mathscr{I}_{v,0}, \mathscr{E}_0) + \int_0^t f_i\left(t, \mathscr{S}_{an}, \mathscr{I}_{an}, \mathscr{V}_{an}, \mathscr{R}_{an}, \mathscr{S}_{vn}, \mathscr{I}_{vn}, \mathscr{E}_n\right)\ dt \end{aligned} \tag{21}$$

$$\begin{cases} \mathscr{X} = \mathscr{C}\left[0, \mathscr{T}\right] \\ \mathscr{T} : \mathscr{X} \longrightarrow \mathscr{X} \\ \mathscr{T}(\mathscr{U}) = \mathscr{U} \\ \mathscr{T}\left(\mathscr{S}_a, \mathscr{I}_a, \mathscr{V}_a, , \mathscr{R}_a, \mathscr{S}_v, \mathscr{I}_v, \mathscr{E}\right) & = \left(\mathscr{S}_a, \mathscr{I}_a, \mathscr{V}_a, , \mathscr{R}_a, \mathscr{S}_v, \mathscr{I}_v, \mathscr{E}\right). \end{cases} \tag{22}$$

$$\begin{aligned}\left|\mathscr{F}-\overline{\mathscr{F}}\right| \leq \mathscr{L}_F\mathscr{T}\left[\left\|\mathscr{S}_a-\bar{\mathscr{S}}_a\right\|+\left\|\mathscr{I}_a-\bar{\mathscr{I}}_a\right\|+\left\|\mathscr{V}_a-\bar{\mathscr{V}}_a\right\|\right. \\ \left.+\left\|\mathscr{R}_a-\bar{\mathscr{R}}_a\right\|+\left\|\mathscr{S}_v-\bar{\mathscr{S}}_v\right\|+\left\|\mathscr{I}_v-\bar{\mathscr{I}}_v\right\|+\left\|\mathscr{E}-\bar{\mathscr{E}}\right\|\right].\end{aligned} \tag{23}$$

If $\mathscr{L}_F\mathscr{T}>1$, $\mathscr{T}$ has a unique fixed point, so model has a unique solution. Let use D to represents in there domain $|t-t_0|\leq a$ and $\|\mathscr{U}-\mathscr{U}_0\|\leq b$, where $\mathscr{U}=(\mathscr{S}_a,\mathscr{I}_a,\mathscr{V}_a,,\mathscr{R}_a,\mathscr{S}_v,\mathscr{I}_v,\mathscr{E})$, $\mathscr{U}_0=(\mathscr{S}_a(0),\mathscr{I}_a(0),\mathscr{V}_a(0),\mathscr{R}_a(0),\mathscr{S}_v(0),\mathscr{I}_v(0),\mathscr{E}(0))$ and consider $\mathscr{F}(t,\mathscr{U}(t))$, satisfies Lipschitz conditions, $\|f(t,\mathscr{S}_a(t))-f(t,\mathscr{I}_a(t))\|\leq K\|\mathscr{S}_a(t)-\mathscr{I}_a(t)\|$ and where this pairs $(t,\mathscr{S}_a(t))$ and $(t,\mathscr{I}_a(t))$ it contain in the domain D, in which the symbol K denotes a positive constant.

So there exist a positive constant $\delta>0$ there is exactly one solution vector $\mathscr{U}(t)$ of the system

$$\mathscr{F}(t,\mathscr{U}(t))=\begin{cases} f_1(t,\mathscr{U}) &= f_1\left(t,\mathscr{S}_a,\mathscr{I}_a,\mathscr{V}_a,,\mathscr{R}_a,\mathscr{S}_v,\mathscr{I}_v,\mathscr{E}\right)\\ f_2(t,\mathscr{U}) &= f_3\left(t,\mathscr{S}_a,\mathscr{I}_a,\mathscr{V}_a,,\mathscr{R}_a,\mathscr{S}_v,\mathscr{I}_v,\mathscr{E}\right)\\ f_3(t,\mathscr{U}) &= f_3\left(t,\mathscr{S}_a,\mathscr{I}_a,\mathscr{V}_a,,\mathscr{R}_a,\mathscr{S}_v,\mathscr{I}_v,\mathscr{E}\right)\\ f_4(t,\mathscr{U}) &= f_4\left(t,\mathscr{S}_a,\mathscr{I}_a,\mathscr{V}_a,,\mathscr{R}_a,\mathscr{S}_v,\mathscr{I}_v,\mathscr{E}\right)\\ f_5(t,\mathscr{U}) &= f_5\left(t,\mathscr{S}_a,\mathscr{I}_a,\mathscr{V}_a,,\mathscr{R}_a,\mathscr{S}_v,\mathscr{I}_v,\mathscr{E}\right)\\ f_6(t,\mathscr{U}) &= f_6\left(t,\mathscr{S}_a,\mathscr{I}_a,\mathscr{V}_a,,\mathscr{R}_a,\mathscr{S}_v,\mathscr{I}_v,\mathscr{E}\right)\\ f_7(t,\mathscr{U}) &= f_7\left(t,\mathscr{S}_a,\mathscr{I}_a,\mathscr{V}_a,,\mathscr{R}_a,\mathscr{S}_v,\mathscr{I}_v,\mathscr{E}\right), \end{cases} \tag{24}$$

and $\mathscr{U}(0)=\mathscr{U}_0=(\mathscr{S}_a(0),\mathscr{I}_a(0),\mathscr{V}_a(0),\mathscr{R}_a(0),\mathscr{S}_v(0),\mathscr{I}_v(0),\mathscr{E}(0))$ in the interval $|t-t_0|\leq\delta$. It is also important to note $\|f(t,\mathscr{S}_a(t))-f(t,\mathscr{I}_a(t))\|\leq K\|\mathscr{S}_a-\mathscr{I}_a\|$ is hold by requirement that:

$$\frac{\partial f_i}{\partial\mathscr{U}_j}\quad i,j\quad=1,...,7,$$

it is continuous and limited within the domain D.

Lemma 4. *If $f(t,\mathscr{U})$ is continuous partial derivative $\frac{\partial f_i}{\partial\mathscr{U}_j}$ in a bounded closed convex domain R (i.e., convex set in real numbers), where R is used to represent a real numbers, then it is hold the Lipschitz condition in R is our interested domain: $1\leq\varepsilon\leq R$. So we look to the bounded solution in the from $0\leq R\leq\infty$.*

Theorem 1. *If the domain D represents the region defined in $|t-t_0|\leq a$, and $\|\mathscr{U}-\mathscr{U}_0\|\leq b$ where $\mathscr{U}=(\mathscr{S}_a,\mathscr{I}_a,\mathscr{V}_a,,\mathscr{R}_a,\mathscr{S}_v,\mathscr{I}_v,\mathscr{E})$, $\mathscr{U}_0=(\mathscr{S}_a(0),\mathscr{I}_a(0),\mathscr{V}_a(0),\mathscr{R}_a(0),\mathscr{S}_v(0),\mathscr{I}_v(0),\mathscr{E}(0))$ is bounded such that $\|f(t,\mathscr{S}_a(t))-f(t,\mathscr{I}_a(t))\|\leq K\|\mathscr{S}_a(t)-\mathscr{I}_a(t)\|$ holds where $1\leq\varepsilon\leq R$. Then solution of model exist a in equation $\frac{d\mathscr{S}_a}{dt},\frac{d\mathscr{I}_a}{dt},\frac{d\mathscr{V}_a}{dt},\frac{d\mathscr{R}_a}{dt},\frac{d\mathscr{S}_v}{dt},\frac{d\mathscr{I}_v}{dt},\frac{d\mathscr{E}}{dt}$ which is closed in the domain D.*

Proof. To show that solution of the system in the domain D is bounded, we get

$$\begin{cases} f_1 &= (1-k)M_1 - \beta_a \mathscr{S}_a \mathscr{I}_v - \beta_b \mathscr{S}_a \mathscr{E} - \beta_c \mathscr{S}_a \mathscr{I}_a - \mu \mathscr{S}_a - v_1 \mathscr{S}_a + v_2 \mathscr{V}_a \\ f_2 &= \beta_a \mathscr{S}_a \mathscr{I}_v + \beta_b \mathscr{S}_a \mathscr{E} + \beta_c \mathscr{S}_a \mathscr{I}_a - (\delta + \mu)\mathscr{I}_a \\ f_3 &= kM_1 + v_1 \mathscr{S}_a - v_2 \mathscr{V}_a - \mu \mathscr{V}_a \\ f_4 &= \delta \mathscr{I}_a - \mu \mathscr{R}_a \\ f_5 &= M_2 - \frac{\beta_4 \mathscr{S}_v \mathscr{I}_a}{\mathscr{N}_a} - \mu_v \mathscr{S}_v \\ f_6 &= \frac{\beta_4 \mathscr{S}_v \mathscr{I}_a}{\mathscr{N}_a} - \mu_v \mathscr{I}_v \\ f_7 &= \phi \mathscr{I}_a - \omega \mathscr{E}. \end{cases} \tag{25}$$

We show that

$$\frac{\partial f_i}{\partial \mathscr{U}_j} \quad i,j \quad = 1, ..., 7,$$

are well-defined in limited meaning their partial derivatives is remain continuous and bounded. We analyzed the partial derivatives of all the model.

From equation (25) take f_1 :

$$\begin{cases} \frac{\partial f_1}{\partial \mathscr{S}_a} &= -\beta_a \mathscr{I}_v - \beta_b \mathscr{E} - \beta_c \mathscr{I}_a - \mu - v_1, \\ \left|\frac{\partial f_1}{\partial \mathscr{S}_a}\right| &= |-\beta_a \mathscr{I}_v - \beta_b \mathscr{E} - \beta_c \mathscr{I}_a - \mu - v_1| < \infty \\ \frac{\partial f_1}{\partial \mathscr{I}_a} = & -\beta_c \mathscr{S}_a, \\ \left|\frac{\partial f_1}{\partial \mathscr{I}_a}\right| &= |-\beta_c \mathscr{S}_a| < \infty \\ \frac{\partial f_1}{\partial \mathscr{V}_a} &= v_2, \\ \left|\frac{\partial f_1}{\partial \mathscr{V}_a}\right| &= |v_2| < \infty \\ \frac{\partial f_1}{\partial \mathscr{R}_a} &= 0, \\ \left|\frac{\partial f_1}{\partial \mathscr{R}_a}\right| &= |0| < \infty \\ \frac{\partial f_1}{\partial \mathscr{S}_v} &= 0, \\ \left|\frac{\partial f_1}{\partial \mathscr{S}_v}\right| &= |0| < \infty \\ \frac{\partial f_1}{\partial \mathscr{I}_v} &= -\beta_a \mathscr{S}_a, \\ \left|\frac{\partial f_1}{\partial \mathscr{I}_v}\right| &= |-\beta_a \mathscr{S}_a| < \infty \\ \frac{\partial f_1}{\partial \mathscr{E}} &= -\beta_b \mathscr{S}_a, \\ \left|\frac{\partial f_1}{\partial \mathscr{E}}\right| &= |-\beta_b \mathscr{S}_a| < \infty. \end{cases} \tag{26}$$

From equation (25) take f_2 :

$$\begin{cases} \left|\frac{\partial f_2}{\partial \mathscr{S}_a}\right| & = |\beta_a \mathscr{I}_v + \beta_b \mathscr{E} + \beta_c \mathscr{I}_a| < \infty \\ \left|\frac{\partial f_2}{\partial \mathscr{I}_a}\right| & = |\beta_c \mathscr{S}_a - (\delta + \mu)| < \infty \\ \left|\frac{\partial f_2}{\partial \mathscr{V}_a}\right| & = |0| < \infty \\ \left|\frac{\partial f_2}{\partial \mathscr{R}_a}\right| & = |0| < \infty \\ \left|\frac{\partial f_2}{\partial \mathscr{S}_v}\right| & = |0| < \infty \\ \left|\frac{\partial f_2}{\partial \mathscr{I}_v}\right| & = |\beta_a \mathscr{S}_a| < \infty \\ \left|\frac{\partial f_2}{\partial \mathscr{E}}\right| & = |\beta_b \mathscr{S}_a| < \infty \end{cases} \tag{27}$$

From equation (25) take f_3 :

$$\begin{cases} \left|\frac{\partial f_3}{\partial \mathscr{S}_a}\right| & = |v_1| < \infty \\ \left|\frac{\partial f_3}{\partial \mathscr{I}_a}\right| & = |0| < \infty \\ \left|\frac{\partial f_3}{\partial \mathscr{V}_a}\right| & = |-\mu - v_1| < \infty \\ \left|\frac{\partial f_3}{\partial \mathscr{R}_a}\right| & = |0| < \infty \\ \left|\frac{\partial f_3}{\partial \mathscr{S}_v}\right| & = |0| < \infty \\ \left|\frac{\partial f_3}{\partial \mathscr{I}_v}\right| & = |0| < \infty \\ \left|\frac{\partial f_3}{\partial \mathscr{E}}\right| & = |0| < \infty \end{cases} \tag{28}$$

From equation (25) take f_4 :

$$\begin{cases} \left|\frac{\partial f_4}{\partial \mathscr{S}_a}\right| & = |0| < \infty \\ \left|\frac{\partial f_4}{\partial \mathscr{I}_a}\right| & = |\delta| < \infty \\ \left|\frac{\partial f_4}{\partial \mathscr{V}_a}\right| & = |0| < \infty \\ \left|\frac{\partial f_4}{\partial \mathscr{R}_a}\right| & = |-\mu| < \infty \\ \left|\frac{\partial f_4}{\partial \mathscr{S}_v}\right| & = |0| < \infty \\ \left|\frac{\partial f_4}{\partial \mathscr{I}_v}\right| & = |0| < \infty \\ \left|\frac{\partial f_4}{\partial \mathscr{E}}\right| & = |\ 0\ | \prec \infty \end{cases} \tag{29}$$

From equation (25) take f_5 :

$$\begin{cases} \left|\frac{\partial f_5}{\partial \mathscr{S}_a}\right| & = |0| < \infty \\ \left|\frac{\partial f_5}{\partial \mathscr{I}_a}\right| & = \left|-\frac{\beta_4 \mathscr{S}_v}{\mathscr{N}_a}\right| < \infty \\ \left|\frac{\partial f_5}{\partial \mathscr{V}_a}\right| & = |0| < \infty \\ \left|\frac{\partial f_5}{\partial \mathscr{R}_a}\right| & = |0| < \infty \\ \left|\frac{\partial f_5}{\partial \mathscr{S}_v}\right| & = \left|-\frac{\beta_4 I_a}{\mathscr{N}_a} - \mu_v\right| < \infty \\ \left|\frac{\partial f_5}{\partial \mathscr{I}_v}\right| & = |0| < \infty \\ \left|\frac{\partial f_5}{\partial \mathscr{E}}\right| & = |0| < \infty \end{cases} \tag{30}$$

From equation (25) take f_6 :

$$\begin{cases} \left|\frac{\partial f_6}{\partial \mathscr{S}_a}\right| & = |0| < \infty \\ \left|\frac{\partial f_6}{\partial \mathscr{I}_a}\right| & = \left|\frac{\beta_4 S_v}{\mathscr{N}_a}\right| < \infty \\ \left|\frac{\partial f_6}{\partial \mathscr{V}_a}\right| & = |0| < \infty \\ \left|\frac{\partial f_6}{\partial \mathscr{R}_a}\right| & = |0| < \infty \\ \left|\frac{\partial f_6}{\partial \mathscr{S}_v}\right| & = \left|\frac{\beta_4 \mathscr{I}_a}{\mathscr{N}_a}\right| < \infty \\ \left|\frac{\partial f_6}{\partial \mathscr{I}_v}\right| & = |-\mu_v| < \infty \\ \left|\frac{\partial f_6}{\partial \mathscr{E}}\right| & = |0| < \infty \end{cases} \tag{31}$$

Finally from equation (25) take f_7 :

$$\begin{cases} \left|\frac{\partial f_7}{\partial \mathscr{S}_a}\right| & = |0| < \infty \\ \left|\frac{\partial f_7}{\partial \mathscr{I}_a}\right| & = |\phi| < \infty \\ \left|\frac{\partial f_7}{\partial \mathscr{V}_a}\right| & = |0| < \infty \\ \left|\frac{\partial f_7}{\partial \mathscr{R}_a}\right| & = |0| < \infty \\ \left|\frac{\partial f_7}{\partial \mathscr{S}_v}\right| & = |0| < \infty \\ \left|\frac{\partial f_7}{\partial \mathscr{I}_v}\right| & = |0| < \infty \\ \left|\frac{\partial f_7}{\partial \mathscr{E}}\right| & = |-\omega| < \infty \end{cases} \tag{32}$$

It has been clearly established that all the partial derivatives are continuous and limited in value, therefor according to Theorem 1, we can concluded that a solution is unique $f_1, f_2, f_3, f_4, f_5, f_6, f_7$ in the domain D.

2.4. Disease Free Equilibrium Points (DFE)

To determine in the DFE $\mathfrak{E}$ of model (2.1), each equation on the right-hand side in the model (2) is equal to zero. After simplifying and arranging the expressions,

$$\begin{cases} (1-k)M_1 - \beta_a \mathscr{S}_a \mathscr{I}_v - \beta_b \mathscr{S}_a \mathscr{E} - \beta_c \mathscr{S}_a \mathscr{I}_a - \mu \mathscr{S}_a - v_1 \mathscr{S}_a + v_2 \mathscr{V}_a = 0 \\ \beta_a \mathscr{S}_a \mathscr{I}_v + \beta_b \mathscr{S}_a \mathscr{E} + \beta_c \mathscr{S}_a \mathscr{I}_a - (\delta+\mu)\mathscr{I}_a = 0 \\ kM_1 + v_1 \mathscr{S}_a - v_2 \mathscr{V}_a - \mu \mathscr{V}_a = 0 \\ \delta \mathscr{I}_a - \mu \mathscr{R}_a = 0 \\ M_2 - \frac{\beta_4 \mathscr{S}_v \mathscr{I}_a}{\mathscr{N}_a} - \mu_v \mathscr{S}_v = 0 \\ \frac{\beta_4 \mathscr{S}_v \mathscr{I}_a}{\mathscr{N}_a} - \mu_v \mathscr{I}_v = 0 \\ \phi \mathscr{I}_a - \omega \mathscr{E} = 0, \end{cases} \tag{33}$$

we obtain

$$\mathfrak{E} = (\tfrac{(1-k)M_1}{\mu}, \quad 0, \quad \tfrac{\mu k+(1-k)M_1}{\mu^2}, \quad 0, \quad \tfrac{M_2}{\mu_v}, \quad 0, \quad 0) \tag{34}$$

2.5. Endemic Point of Equilibrium (EEP)

In here we analyze the existence of the equilibrium points in the LSD model (2), shown by $\mathfrak{E}^*$ and is given below:

$$\begin{cases} (1-k)M_1 - \beta_a \mathscr{S}_a^* \mathscr{I}_v^* - \beta_b \mathscr{S}_a^* \mathscr{E}^* - \beta_c \mathscr{S}_a^* \mathscr{I}_a^* - \mu \mathscr{S}_a^* - v_1 \mathscr{S}_a^* + v_2 \mathscr{V}_a^* = 0 \\ \beta_a \mathscr{S}_a^* \mathscr{I}_v^* + \beta_b \mathscr{S}_a^* \mathscr{E}^* + \beta_c \mathscr{S}_a^* \mathscr{I}_a^* - (\delta+\mu)\mathscr{I}_a^* = 0 \\ kM_1 + v_1 \mathscr{S}_a^* - v_2 \mathscr{V}_a^* - \mu \mathscr{V}_a^* = 0 \\ \delta \mathscr{I}_a^* - \mu \mathscr{R}_a = 0 \\ M_2 - \frac{\beta_4 \mathscr{S}_v^* \mathscr{I}_a^*}{\mathscr{N}_a^*} - \mu_v \mathscr{S}_v^* = 0 \\ \frac{\beta_4 \mathscr{S}_v^* \mathscr{I}_a^*}{\mathscr{N}_a^*} - \mu_v \mathscr{I}_v^* = 0 \\ \phi \mathscr{I}_a^* - \omega \mathscr{E}^* = 0 \end{cases} \tag{35}$$

$$\mathfrak{E}^* = (a, \quad b, \quad c, \quad d, \quad f, \quad g) \tag{36}$$

where $a = \frac{(1-k)M_1+v_2V_a}{\lambda^*+\mu+V_1}$, $b = \frac{-\beta_a \mathscr{S}_a^* \mathscr{I}_V^* - \beta_b \mathscr{S}_a^* \mathscr{E}^*}{\beta_c \mathscr{S}_a^* - (\delta+\mu)}$, $c = \frac{(kM_1 + v_1(\frac{(1-k)M_1}{\lambda^*+\mu}) + (\frac{-\beta_a \mathscr{S}_a^* \mathscr{I}_v^* - \beta_b \mathscr{S}_a^* \mathscr{E}^*}{\beta_c \mathscr{S}_a^* - \delta - \mu - v_2}))}{\mu - v_2}$, $d = \frac{\delta}{\mu}\left(\frac{-\delta\beta_a \mathscr{S}_a^* \mathscr{I}_v^* - \beta_b \mathscr{S}_a^* \mathscr{E}^*}{(\mu\beta_c \mathscr{S}_a^* - \mu\delta - \mu^2 - \mu)}\right)$, $e = \frac{M_2}{\beta_4 \mathscr{I}_a^* + \mathscr{N}_a^* \mu_v}$, $f = \frac{\beta_4 \mathscr{S}_v^* \mathscr{I}_a^*}{\mu_v \mathscr{N}_a^*}$, and $g = \frac{\phi \mathscr{I}_a^*}{\omega}$.

2.6. Basic Reproductive Number

Applying the next generation matrix approach to our model (2) the basic reproduction number can be determined by analyzing the following generation matrix, $\mathscr{F}$ and $\mathscr{V}$, that is the jacobian matrices associated to the rate of appearance of new infections and the net

rate out of the corresponding compartments.

$$\begin{aligned}
\mathscr{F} &= \begin{bmatrix} 0 & \frac{-\beta_c(1-k)M_1}{\mu} \\ 0 & \frac{\beta_c(1-k)M_1}{\mu} \end{bmatrix} \\
\mathscr{V} &= \begin{bmatrix} -\mu - v_1 & 0 \\ 0 & -(\delta+\mu) \end{bmatrix} \\
\mathscr{F}\mathscr{V}^{-1} &= \begin{bmatrix} 0 & \frac{-\beta_c(1-k)M_1}{\mu} \\ 0 & \frac{\beta_c(1-k)M_1}{\mu} \end{bmatrix} \begin{bmatrix} \frac{1}{-\mu-v_1} & 0 \\ 0 & \frac{-\mu-v_1}{\mu(\delta+\mu)} \end{bmatrix} \\
\mathscr{F}\mathscr{V}^{-1} &= \begin{bmatrix} 0 & \frac{(1-k)M_1\beta_c}{\mu(\delta+\mu)} \\ 0 & \frac{-\beta_c(1-k)M_1}{\mu(\delta+\mu)} \end{bmatrix} \\
R_0^v &= \frac{\beta_c(1-k)M_1(\mu+v_1)}{\mu^*(\delta+\mu)}
\end{aligned} \tag{37}$$

If $v_1 = 0$, then $R_0 = \frac{\beta_c(1-k)M_1(\mu)}{\mu^2(\delta+\mu)}$.

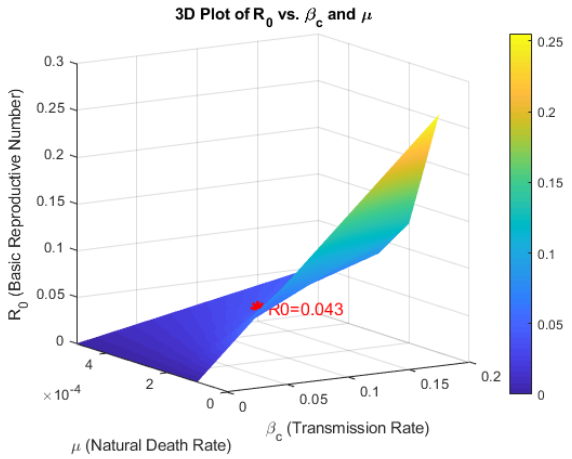

Figure 2: sensitivity pi-chart of R_0

.

If $v_1 = 0$, then $R_0 = \frac{\beta_c(1-k)M_1}{\mu(\delta+\mu)}$.

2.7. Sensitivity Analysis

This section we are analyze the most sensitive term in the LSD model.

$$\begin{aligned}
S_P^{R_0} &= \frac{P}{R_0} \times \frac{\partial R_0}{\partial P} \\
S_{\beta_c}^{R_0} &= 1 \\
S_k^{R_0} &= \frac{-k}{1-k} = -0.2340 \\
S_{M_1}^{R_0} &= 1
\end{aligned}$$

$$\begin{aligned} S_{v_1}^{R_0} &= 1 \\ S_{\mu}^{R_0} &= (-1)(\frac{\delta + 2\mu + 1}{\delta + \mu + 1} = -0.9990) \\ S_{\delta}^{R_0} &= \frac{-\delta}{(\delta + \mu + 1)} = -0.0714 \end{aligned}$$

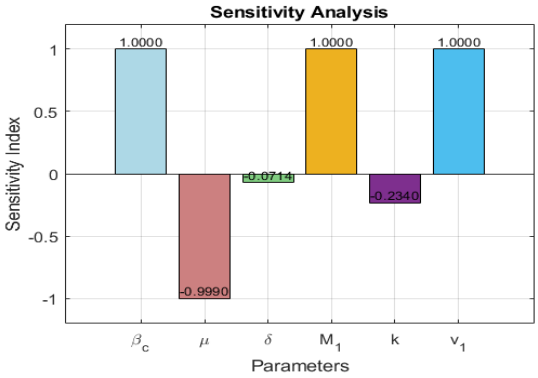

Figure 3: sensitivity bar-chart of R_0

2.8. Local Stability

2.8.1. Local Stability

Local stability of the disease-free equilibrium (DFE) implies that if the disease is initially rare, it will die out when the basic reproduction number $R_0 < 1$.

We begin by analyzing the local stability at disease free equilibrium point $\mathfrak{E}$. Before continuing the following points need to be considered in Theorem 2.

Theorem 2. *The model (1) is locally asymptotically stable at $\mathfrak{E}$ with in ξ when $R_0 < 1$ and if $R_0 > 1$ then it is unstable*

Proof.

$$J(\mathfrak{E}^*) - \lambda I =$$

$$\begin{bmatrix} -\mu - \lambda - v_1 + v2 & 0 & 0 & 0 & 0 & \frac{\beta_a(1-k)M_1}{\mu} & \frac{-\beta_b(1-k)M_1}{\mu} \\ 0 & \frac{\beta_c(1-k)M_1 - \mu\delta - \mu^2 - \mu}{\mu} - \lambda & 0 & 0 & 0 & -\frac{\beta_a(1-k)M_1}{\mu} & \frac{\beta_b(1-k)M_1}{\mu} \\ v_1 & v_2 & -\mu - \lambda & 0 & 0 & 0 & 0 \\ 0 & \delta & 0 & -\mu - \lambda & 0 & 0 & 0 \\ 0 & \frac{-\beta_4 M_2}{\mu_v \mathcal{N}_a} & 0 & 0 & -\mu_v - \lambda & 0 & 0 \\ 0 & \frac{\beta_4 M_2}{\mu_v \mathcal{N}_a} & 0 & 0 & 0 & -\mu_v - \lambda & 0 \\ 0 & \phi & 0 & 0 & 0 & 0 & -\omega - \lambda \end{bmatrix}$$

In column first eigen value $\lambda_1 = -\mu - v_1 + v_2$. The reduced matrix is now given below

$$\begin{bmatrix} -\mu-\lambda & 0 & 0 & 0 & \frac{\beta_a(1-k)M_1}{\mu} & \frac{-\beta_b(1-k)M_1}{\mu} \\ 0 & \frac{\beta_c(1-k)M_1-\mu\delta-\mu^2-\mu v_2}{\mu}-\lambda & 0 & 0 & -\frac{\beta_a(1-k)M_1}{\mu} & \frac{\beta_b(1-k)M_1}{\mu} \\ 0 & \delta & -\mu-\lambda & 0 & 0 & 0 \\ 0 & \frac{-\beta_4 M_2}{\mu_v \mathcal{N}_a} & 0 & -\mu_v-\lambda & 0 & 0 \\ 0 & \frac{\beta_4 M_2}{\mu_v \mathcal{N}_a} & 0 & 0 & -\mu_v-\lambda & 0 \\ 0 & \phi & 0 & 0 & 0 & -\omega-\lambda \end{bmatrix}$$

In first column the second eigen value $\lambda_2 = -\mu$. The reduced matrix is now given below

$$\begin{bmatrix} \frac{\beta_c(1-k)M_1-\mu\delta-\mu^2-\mu v_2}{\mu}-\lambda & 0 & 0 & -\frac{\beta_a(1-k)M_1}{\mu} & \frac{\beta_b(1-k)M_1}{\mu} \\ \delta & -\mu-\lambda & 0 & 0 & 0 \\ \frac{-\beta_4 M_2}{\mu_v \mathcal{N}_a} & 0 & -\mu_v-\lambda & 0 & 0 \\ \frac{\beta_4 M_2}{\mu_v \mathcal{N}_a} & 0 & 0 & -\mu_v-\lambda & 0 \\ \phi & 0 & 0 & 0 & -\omega-\lambda \end{bmatrix}$$

From third column the third eigen value $\lambda_3 = -\mu_v$. The reduced matrix is now given below

$$\begin{bmatrix} \frac{\beta_c(1-k)M_1-\mu\delta-\mu^2-\mu v_2}{\mu}-\lambda & 0 & -\frac{\beta_a(1-k)M_1}{\mu} & \frac{\beta_b(1-k)M_1}{\mu} \\ \delta & -\mu-\lambda & 0 & 0 \\ \frac{\beta_4 M_2}{\mu_v \mathcal{N}_a} & 0 & -\mu_v-\lambda & 0 \\ \phi & 0 & 0 & -\omega-\lambda \end{bmatrix}$$

From second column the fourth eigen value $\lambda_4 = -\mu$. The reduced matrix is now given below

$$\begin{bmatrix} \frac{\beta_c(1-k)M_1-\mu\delta-\mu^2-\mu v_2}{\mu}-\lambda & -\frac{\beta_a(1-k)M_1}{\mu} & \frac{\beta_b(1-k)M_1}{\mu} \\ \frac{\beta_4 M_2}{\mu_v N_a} & -\mu_v-\lambda & 0 \\ \phi & 0 & -\omega-\lambda \end{bmatrix}$$

Using Mathematica the rest of the eigen values are obtained as follow:

$$\lambda_5 = -\omega, \lambda_6 = -\mu_v, \lambda_7 = -\left(-(\delta+\mu+v_2\right)^2.$$

It is clear from the above equation the $R_0 < 1$, which show that at the system remains stable in a local neighborhood of the equilibrium point.

2.9. Global Stability

2.9.1. Global Stability

Global stability indicates that, regardless of initial infection levels, the disease will ultimately be eradicated when $R_0 < 1$, reflecting effective long-term disease control.

2.9.2. Equilibrium Point of Disease Free

Here in this model number of uninfected compartment (healthy cattle) is represented by $\mathscr{B} \in R_+^m$ and number of infected compartment is shown by $\mathscr{Q} \in R_+^n$.

$$\frac{d\mathscr{B}}{dt} = F(\mathscr{B}, \mathscr{Q}), \frac{d\mathscr{Q}}{dt} = G(\mathscr{B}, 0), G(\mathscr{B}, 0) = 0. \tag{38}$$

and the equilibrium point in the absence of disease is represented by $\mathfrak{E}^* = (\mathscr{B}^0, 0)$.
(H_1) . $\frac{d\mathscr{B}}{dt} = F(\mathscr{B}, 0)$, $\mathscr{B}^0$ is globally asymptotically stable.
(H_2) . $G(\mathscr{B}, Q) = X\mathscr{Q} - G(\mathscr{B}, \mathscr{Q}), G(\mathscr{B}, \mathscr{Q}) \geq 0$, for $G(\mathscr{B}, \mathscr{Q}) \in \Omega$.

Theorem 3. *The system globally asymptotically stable for a disease-free equilibrium if* $R_0 < 1$ *and it is unstable if* $R_0 > 1$.

Proof. An alternative method in the system of the model (1) of LSD to express in following: $\mathscr{B} = (\mathscr{S}_a, \mathscr{V}_a, \mathscr{R}_a, \mathscr{S}_v, \mathscr{I}_v, \mathscr{E}) \in R^5$ and $= \left(\frac{(1-k)M_1}{\mu}, \frac{\mu k+(1-k)M_1}{\mu^2}, 0, \frac{M_2}{\mu_v}, 0\right)$. Now we have

$$\frac{d\mathscr{B}}{dt} = \begin{cases} (1-k)M_1 - \beta_a \mathscr{S}_a \mathscr{I}_v - \beta_b \mathscr{S}_a \mathscr{E} - \beta_c \mathscr{S}_a \mathscr{I}_a - \mu \mathscr{S}_a - v_1 \mathscr{S}_a + v_2 \mathscr{V}_a \\ kM_1 + v_1 \mathscr{S}_a - v_2 \mathscr{V}_a - \mu \mathscr{V}_a \\ \delta \mathscr{I}_a - \mu \mathscr{R}_a \\ M_2 - \frac{\beta_4 \mathscr{S}_v \mathscr{I}_a}{\mathscr{N}_a} - \mu_v \mathscr{S}_v \\ \phi \mathscr{I}_a - \omega \mathscr{E} \end{cases} \tag{39}$$

$$\mathscr{B}^0 = \left(\frac{(1-k)M_1}{\mu}, \frac{\mu k+(1-k)M_1}{\mu^2}, 0, \frac{M_2}{\mu_v}, 0\right)$$

$$\frac{d\mathscr{B}}{dt} = F(\mathscr{B}^0, 0) = \begin{cases} \frac{(1-k)M_1}{\mu} \\ \frac{\mu k+(1-k)M_1}{\mu^2} \\ 0 \\ \frac{M_2}{\mu_v} \\ 0 \end{cases}$$

$F(\mathscr{B}^0, 0)$ has a distinct point of equilibrium $\mathscr{B}^0 = \left(\frac{(1-k)M_1}{\mu}, \frac{\mu k+(1-k)M_1}{\mu^2}, \frac{M_2}{\mu_v}\right)$, which has asymptotically global stable. Thus H_1 hold.

For second condition H_2:

$$\widetilde{G}(\mathscr{B}, \mathscr{Q}) = \begin{cases} \beta_a \mathscr{S}_a \mathscr{I}_v + \beta_b \mathscr{S}_a \mathscr{E} + \beta_c \mathscr{S}_a \mathscr{I}_a - (\delta + \mu)\mathscr{I}_a \\ \frac{\beta_4 \mathscr{S}_v \mathscr{I}_a}{\mathscr{N}_a} - \mu_v \mathscr{I}_v \end{cases}$$

Then we get

$$X = A_1(\mathscr{B}^0, 0) = \begin{pmatrix} -(\delta+\mu)+\beta_c\mathscr{S}_a^0 & \beta_a\mathscr{S}_a^0 \\ \frac{\beta_4\mathscr{S}_v^0}{\mathscr{N}_a}, & -\mu_v \end{pmatrix}.$$

In the matrix X is evidently represents an M-matrix, now its upper diagonal entries are not less than zero. Thus

$$\begin{aligned}
\widetilde{G}(\mathscr{B},\mathscr{Q}) &= XA - G(\mathscr{B},\mathscr{Q}) \\
&= \begin{pmatrix} -(\delta+\mu)+\beta_c\mathscr{S}_a^0 & \beta_a\mathscr{S}_a^0 \\ \frac{\beta_4\mathscr{S}_v^0}{\mathscr{N}_a}, & -\mu_v \end{pmatrix}\begin{pmatrix} \mathscr{I}_a \\ \mathscr{I}_v \end{pmatrix} - \begin{pmatrix} \beta_a\mathscr{S}_a\mathscr{I}_v + \beta_b\mathscr{S}_a\mathscr{E} + \beta_c\mathscr{S}_a\mathscr{I}_a \\ -(\delta+\mu)\mathscr{I}_a \\ \frac{\beta_4\mathscr{S}_v\mathscr{I}_a}{\mathscr{N}_a} - \mu_v\mathscr{I}_v \end{pmatrix} \\
&= \begin{pmatrix} -(\delta+\mu)\mathscr{I}_a + \beta_c\mathscr{S}_a^0\mathscr{I}_a + \beta_a\mathscr{S}_a^0\mathscr{I}_v \\ \frac{\beta_4\mathscr{S}_v^0\mathscr{I}_a}{\mathscr{N}_a} - -\mu_v\mathscr{I}_v \end{pmatrix} + \begin{pmatrix} -\beta_a\mathscr{S}_a\mathscr{I}_v - \beta_b\mathscr{S}_a\mathscr{E} - \beta_c\mathscr{S}_a \\ \mathscr{I}_a + (\delta+\mu)\mathscr{I}_a \\ -\frac{\beta_4\mathscr{S}_v\mathscr{I}_a}{\mathscr{N}_a} + \mu_v\mathscr{I}_v \end{pmatrix} \\
&= \begin{pmatrix} (\beta_c\mathscr{I}_a + \beta_b\mathscr{I}_v)\,\mathscr{S}_a^0 - (\beta_a\mathscr{I}_v + \beta_c\mathscr{I}_a) \\ \mathscr{S}_a - \beta_b\mathscr{E}\mathscr{S}_a \\ 0 \end{pmatrix} \\
&= \begin{pmatrix} (\beta_c\mathscr{I}_a + \beta_b\mathscr{I}_v)\left(\mathscr{S}_a^0 - \mathscr{S}_a\right) - \beta_b\mathscr{E}\mathscr{S}_a \\ 0 \end{pmatrix}.
\end{aligned}$$

Hence $\mathscr{S}_a^0 > \mathscr{S}_a$, $\mathscr{B}^0 = \left(\frac{(1-k)M_1}{\mu}, \frac{\mu k+(1-k)M_1}{\mu^2}, \frac{M_2}{\mu_v}\right) \geq 1$, and $G(\mathscr{B},\mathscr{Q}) \geq 0$ is globally asymptotically stable.

2.9.3. Global Stability of the Endemic Equilibrium Point

In here we use a Lyapnov function to demonstrate the conditions for the global asymptotic stability in the endemic equilibrium point in R_7^+.

Theorem 4. *For system(2) there exist unique endemic equilibrium point $\mathfrak{E}^*$ exist for LSD disease, which in the case where $R_0 > 1$ is globally asymptotically stable, otherwise it is unstable if $R_0 < 1$.*

Proof. Let us consider Lyapnov function

$$\mathscr{F}\left(y_1, y_2, ..., y_n\right) = \Sigma_{i=1}^{n} \frac{1}{2}\left[y_1 - y_i^*\right]^2. \tag{40}$$

For the model (2.1) an example of a positive definite function appears as follows here the i^{th} compartment's population is represented by y_i and point of endemic equilibrium is shown by y_i.

$$\mathscr{F}\left(\mathscr{S}_a, \mathscr{I}_a, \mathscr{V}_a, \mathscr{R}_a, \mathscr{S}_v, \mathscr{I}_v, \mathscr{E}\right) = \Sigma_{i=1}^{7} \frac{1}{2}\left[y_1 - y_i^*\right]^2. \tag{41}$$

For LSD model(1) the Lyapnov function can therefore be written as:

$$\mathscr{F}(x) = \left[(\mathscr{S}_a - \mathscr{S}_a^*)(\mathscr{I}_a - \mathscr{I}_a^*)(\mathscr{V}_a - \mathscr{V}_a^*)(\mathscr{R}_a - \mathscr{R}_a^*)(\mathscr{S}_v - \mathscr{S}_v^*)(\mathscr{I}_v - \mathscr{I}_v^*)(\mathscr{E} - \mathscr{E}^*)\right]^2. \tag{42}$$

$$\begin{aligned}\frac{d\mathscr{F}(x)}{dt} &= [(\mathscr{S}_a-\mathscr{S}_a^*)(\mathscr{I}_a-\mathscr{I}_a^*)(\mathscr{V}_a-\mathscr{V}_a^*)(\mathscr{R}_a-\mathscr{R}_a^*)(\mathscr{S}_v-\mathscr{S}_v^*)(\mathscr{I}_v-\mathscr{I}_v^*)(\mathscr{E}-\mathscr{E}^*)]\\ &\quad \frac{d}{dt}\left(\mathscr{S}_a+\mathscr{I}_a+\mathscr{V}_a+\mathscr{R}_a+\mathscr{S}_v+\mathscr{I}_v+\mathscr{E}\right) \qquad (43)\end{aligned}$$

$$\begin{aligned}\frac{d\mathscr{F}(x)}{dt} &= [\mathscr{S}_a+\mathscr{I}_a+\mathscr{V}_a+\mathscr{R}_a+\mathscr{S}_v+\mathscr{I}_v+\mathscr{E}]-[\mathscr{S}_a^*+\mathscr{I}_a^*+\mathscr{V}_a^*+\mathscr{R}_a^*+\mathscr{S}_v^*+\mathscr{I}_v^*+\mathscr{E}^*]\\ &\quad \frac{d}{dt}\left(\mathscr{S}_a+\mathscr{I}_a+\mathscr{V}_a+\mathscr{R}_a+\mathscr{S}_v+\mathscr{I}_v+\mathscr{E}\right) \qquad (44)\end{aligned}$$

$$\begin{aligned}\frac{d\mathscr{F}(x)}{dt} &= \left[(\mathscr{N}_a+\mathscr{N}_v+\mathscr{E})-\frac{(1-k)M_1+M_2}{\mu+\mu_v+\omega}+\frac{v_1\mathscr{S}_a^*+\phi\mathscr{I}_a^*}{\mu+\mu_v+\omega}\right](\mu+\mu_v+\omega)\\ &\quad \left[(\mathscr{N}_a+\mathscr{N}_v+\mathscr{E})+\frac{(1-k)M_1+M_2}{\mu+\mu_v+\omega}+\frac{v_1\mathscr{S}_a^*+\phi\mathscr{I}_a^*}{\mu+\mu_v+\omega}\right] \qquad (45)\end{aligned}$$

Let $(\mathscr{N}_a+\mathscr{N}_v+\mathscr{E})=\mathscr{N}^*(t)\,\&\,(\mu+\mu_v+\omega)=\xi$

$$\begin{aligned}\frac{d\mathscr{F}(x)}{dt} &\le -\xi\left(\mathscr{N}^*(t)-\frac{(1-k)M_1+M_2}{\xi}+\frac{v_1\mathscr{S}_a^*+\phi\mathscr{I}_a^*}{\xi}\right)\\ &\quad \left(\mathscr{N}^*(t)+\frac{(1-k)M_1+M_2}{\xi}+\frac{v_1\mathscr{S}_a^*+\phi\mathscr{I}_a^*}{\xi}\right) \qquad (46)\end{aligned}$$

$$\frac{d\mathscr{F}(x)}{dt}\le -\xi\left(\mathscr{N}^*(t)-\frac{(1-k)M_1+M_2}{\xi}+\frac{v_1\mathscr{S}_a^*+\phi\mathscr{I}_a^*}{\xi}\right)^2<0 \qquad (47)$$

Consequently, it become shows that $\frac{d\mathscr{V}(x)}{dt}<0$ demonstrating the global asymptotic stability is achieved at the endemic equilibrium is $\mathfrak{E}^*$.

3. Numerical Solution by Euler Method

In this section, numerical solution of the LSD is provided using Euler's method:

$$\begin{cases}\frac{\mathscr{S}_a(t_{n+1})-\mathscr{S}_a(t_n)}{h} &= f_1\left(t_n,(\mathscr{S}_{an},\mathscr{I}_{an},\mathscr{V}_{an},\mathscr{R}_{an},\mathscr{S}_{vn},\mathscr{I}_{vn},\mathscr{E}_n)\right)\\ \frac{\mathscr{I}_a(t_{n+1})-\mathscr{I}_a(t_n)}{h} &= f_2\left(t_n,(\mathscr{S}_{an},\mathscr{I}_{an},\mathscr{V}_{an},\mathscr{R}_{an},\mathscr{S}_{vn},\mathscr{I}_{vn},\mathscr{E}_n)\right)\\ \frac{\mathscr{V}_a(t_{n+1})-\mathscr{V}_a(t_n)}{h} &= f_3\left(t_n,(\mathscr{S}_{an},\mathscr{I}_{an},\mathscr{V}_{an},\mathscr{R}_{an},\mathscr{S}_{vn},\mathscr{I}_{vn},\mathscr{E}_n)\right)\\ \frac{\mathscr{R}_a(t_{n+1})-\mathscr{R}_a(t_n)}{h} &= f_4\left(t_n,(\mathscr{S}_{an},\mathscr{I}_{an},\mathscr{V}_{an},\mathscr{R}_{an},\mathscr{S}_{vn},\mathscr{I}_{vn},\mathscr{E}_n)\right)\\ \frac{\mathscr{S}_v(t_{n+1})-\mathscr{S}_v(t_n)}{h} &= f_5\left(t_n,(\mathscr{S}_{an},\mathscr{I}_{an},\mathscr{V}_{an},\mathscr{R}_{an},\mathscr{S}_{vn},\mathscr{I}_{vn},\mathscr{E}_n)\right)\\ \frac{\mathscr{I}_v(t_{n+1})-\mathscr{I}_v(t_n)}{h} &= f_6\left(t_n,(\mathscr{S}_{an},\mathscr{I}_{an},\mathscr{V}_{an},\mathscr{R}_{an},\mathscr{S}_{vn},\mathscr{I}_{vn},\mathscr{E}_n)\right)\\ \frac{\mathscr{E}(t_{n+1})-\mathscr{E}(t_n)}{h} &= f_7\left(t_n,(\mathscr{S}_{an},\mathscr{I}_{an},\mathscr{V}_{an},\mathscr{R}_{an},\mathscr{S}_{vn},\mathscr{I}_{vn},\mathscr{E}_n)\right),\end{cases} \qquad (48)$$

and

$$\begin{cases} \mathscr{S}_a(t_{n+1}) & = \mathscr{S}_a(t_n) + hf_1\left(t_n, (\mathscr{S}_{an}, \mathscr{I}_{an}, \mathscr{V}_{an}, \mathscr{R}_{an}, \mathscr{S}_{vn}, \mathscr{I}_{vn}, \mathscr{E}_n)\right) \\ \mathscr{I}_a(t_{n+1}) & = \mathscr{I}_a(t_n) + hf_2\left(t_n, (\mathscr{S}_{an}, \mathscr{I}_{an}, \mathscr{V}_{an}, \mathscr{R}_{an}, \mathscr{S}_{vn}, \mathscr{I}_{vn}, \mathscr{E}_n)\right) \\ \mathscr{V}_a(t_{n+1}) & = \mathscr{V}_a(t_n) + hf_3\left(t_n, (\mathscr{S}_{an}, \mathscr{I}_{an}, \mathscr{V}_{an}, \mathscr{R}_{an}, \mathscr{S}_{vn}, \mathscr{I}_{vn}, \mathscr{E}_n)\right) \\ \mathscr{R}_a(t_{n+1}) & = \mathscr{R}_a(t_n) + hf_4\left(t_n, (\mathscr{S}_{an}, \mathscr{I}_{an}, \mathscr{V}_{an}, \mathscr{R}_{an}, \mathscr{S}_{vn}, \mathscr{I}_{vn}, \mathscr{E}_n)\right) \\ \mathscr{S}_v(t_{n+1}) & = \mathscr{S}_v(t_n) + hf_5\left(t_n, (\mathscr{S}_{an}, \mathscr{I}_{an}, \mathscr{V}_{an}, \mathscr{R}_{an}, \mathscr{S}_{vn}, \mathscr{I}_{vn}, \mathscr{E}_n)\right) \\ \mathscr{I}_v(t_{n+1}) & = \mathscr{I}_v(t_n) + hf_6\left(t_n, (\mathscr{S}_{an}, \mathscr{I}_{an}, \mathscr{V}_{an}, \mathscr{R}_{an}, \mathscr{S}_{vn}, \mathscr{I}_{vn}, \mathscr{E}_n)\right) \\ \mathscr{E}(t_{n+1}) & = \mathscr{E}(t_n) + hf_7\left(t_n, (\mathscr{S}_{an}, \mathscr{I}_{an}, \mathscr{V}_{an}, \mathscr{R}_{an}, \mathscr{S}_{vn}, \mathscr{I}_{vn}, \mathscr{E}_n)\right). \end{cases} \tag{49}$$

Further,

$$\begin{cases} \mathscr{S}_a(t_{n+1}) - \mathscr{S}_a(t_n) & = h\left((1-k)M_1 - \beta_a \mathscr{S}_a \mathscr{I}_v - \beta_b \mathscr{S}_a \mathscr{E} - \beta_c \mathscr{S}_a \mathscr{I}_a - \mu \mathscr{S}_a - v_1 \mathscr{S}_a + v_2 \mathscr{V}_a\right) \\ \mathscr{I}_a(t_{n+1}) - \mathscr{I}_a(t_n) & = h\left(\beta_a \mathscr{S}_a \mathscr{I}_v + \beta_b \mathscr{S}_a \mathscr{E} + \beta_c \mathscr{S}_a \mathscr{I}_a - (\delta + \mu)\mathscr{I}_a\right) \\ \mathscr{V}_a(t_{n+1}) - \mathscr{V}_a(t_n) & = h\left(kM_1 + v_1 \mathscr{S}_a - v_2 \mathscr{V}_a - \mu \mathscr{V}_a\right) \\ \mathscr{R}_a(t_{n+1}) - \mathscr{R}_a(t_n) & = h\left(\delta \mathscr{I}_a - \mu \mathscr{R}_a\right) \\ \mathscr{S}_v(t_{n+1}) - \mathscr{S}_v(t_n) & = h\left(M_2 - \frac{\beta_4 \mathscr{S}_v \mathscr{I}_a}{\mathscr{N}_a} - \mu_v \mathscr{S}_v\right) \\ \mathscr{I}_v(t_{n+1}) - \mathscr{I}_v(t_n) & = h\left(\frac{\beta_4 \mathscr{S}_v \mathscr{I}_a}{\mathscr{N}_a} - \mu_v \mathscr{I}_v\right) \\ \mathscr{E}(t_{n+1}) - \mathscr{E}(t_n) & = h\left(\phi \mathscr{I}_a - \omega \mathscr{E}\right). \end{cases} \tag{50}$$

This scheme is now completed.

4. Numerical Results and Discussion

in this section we discuss about numerical simulation of the model.

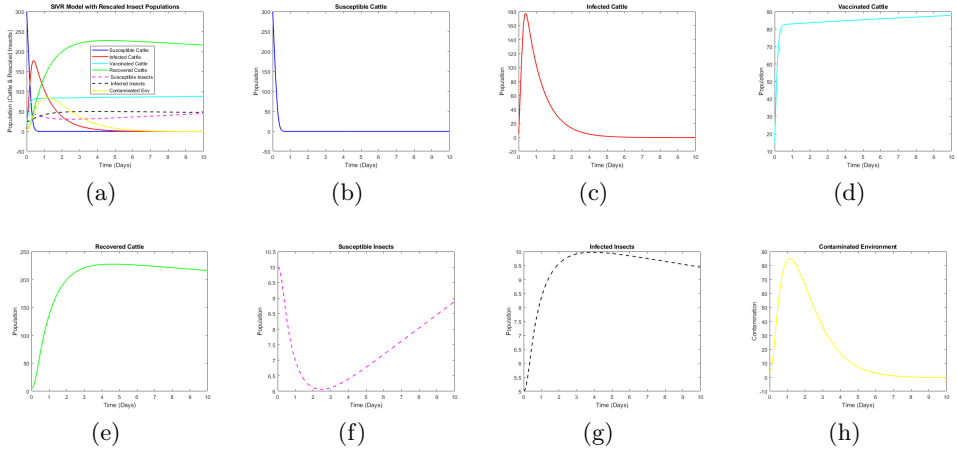

(a) (b) (c) (d)

(e) (f) (g) (h)

Figure 4: Graphical representation of the considered model.

The simulation results presented in plot (a) illustrate the dynamic behavior of the Lumpy Skin Disease (LSD) transmission model using the *SIVR* framework. The plots capture the temporal evolution of cattle populations (susceptible, infected, vaccinated and recovered) the insect vector population (susceptible and infected) and the environmental contamination over time. The results demonstrate the effectiveness of vaccination and recovery in controlling disease prevalence. In this plot shows how the entire system including cattle, insects and environmental virus load evolves over time. The convergence of various compartments toward equilibrium states visually confirms the theoretical findings regarding both local and global stability under certain parameter conditions. This plot (b) shows a gradual decline in the susceptible cattle population over time. This trend is expected as susceptible animals become infected or vaccinated. The introduction of vaccination (via parameter v_1) plays a critical role in reducing the pool of susceptible individuals contributing to disease mitigation. In the plot(c) infected cattle population initially rises as the infection spreads among susceptible animals. However, it reaches a peak and begins to decline indicating the effect of natural recovery δ and the indirect benefits of vaccination and environmental disinfection. The plot (d) for vaccinated cattle compartment shows an increasing trend, which reflects the administration of vaccines to susceptible animals. This increase demonstrates the efficacy of vaccination in reducing the disease burden and confirms the importance of proactive control measures. In plot (e) show a recovered cattle increases over time, highlighting that infected individuals are recovering at a steady rate. This aligns with the recovery rate parameter δ and supports the models assumption that recovered animals acquire lifelong immunity. This plot (f) shows a general decline in the susceptible insect population, which may be due to their exposure to infected cattle and natural death (μ_v). Since insects are key vectors, their reduced population over time is beneficial for controlling LSD spread. The plot(g) of infected insect population rises initially and stabilizes after some time. This behavior mirrors the disease transmission dynamics, as more insects acquire the virus from infected cattle. However without exponential growth the curve suggests the system reaches equilibrium corroborating the models stability analysis. In the plot (h) environmental contamination ($E(t)$) increases due to contributions from infected cattle but eventually levels off due to disinfection efforts (ω). This result emphasizes the role of environmental hygiene and sanitation in managing disease outbreaks.

Symbol	Numerical Values	Symbol	Numerical Values
M_1	1.0 estimated	M_2	0.5estimated
k	1.5	μ	0.01estimated
β_a	0.3	β_b	0.2
β_c	0.0089999	δ	1.008 estimated
μ_v	0.01 estimated		

Table 3: Numerical values of parameters

5. Modeling and Implementation of Optimal Control

Both the calculus of variations and optimal control theory are used to solve optimization problems, and control theory is used to create plans to stop or lessen the spread of LSDV.

(i) The control variables $u_1(t)$ denotes vaccination, aiming to build immunity within the population.Our mane objective to increase the number of individuals who are vaccinated.

(ii) The control variable $u_2(t)$ stands for the treatment of individuals infected with LSDV, the purpose of this control is to decrease the infected population.

Therefore incorporating these two control variables transforms our control problem into a modified version of the system,which is presented below.

$$\begin{cases} \frac{dS_a}{dt} = & (1-k)M_1 - \beta_a \mathscr{S}_a \mathscr{I}_v - \beta_b \mathscr{S}_a \mathscr{E} - \beta_c \mathscr{S}_a \mathscr{I}_a - (u_1(t) + \mu)\mathscr{S}_a - v_1 \mathscr{S}_a + v_2 \mathscr{V}_a \\ \frac{dI_a}{dt} = & \beta_a \mathscr{S}_a \mathscr{I}_v + \beta_b \mathscr{S}_a \mathscr{E} + \beta_c \mathscr{S}_a \mathscr{I}_a - (\delta + \mu)\mathscr{I}_a - (u_2(t))\,\mathscr{I}_a \\ \frac{dV_a}{dt} = & kM_1 + v_1 \mathscr{S}_a - v_2 \mathscr{V}_a - \mu \mathscr{V}_a + u_1(t)\,\mathscr{S}_a \\ \frac{dR_a}{dt} = & \delta \mathscr{I}_a + u_2(t)\,\mathscr{I}_a - \mu \mathscr{R}_a \\ \frac{dS_v}{dt} = & M_2 - \frac{\beta_4 \mathscr{S}_v \mathscr{I}_a}{N_a} - \mu_v \mathscr{S}_v \\ \frac{dI_v}{dt} = & \frac{\beta_4 \mathscr{S}_v \mathscr{I}_a}{N_a} - \mu_v \mathscr{I}_v \\ \frac{dE}{dt} = & \phi \mathscr{I}_a - \omega \mathscr{E} \end{cases} \tag{51}$$

The objective of the control strategies is to minimize the number of susceptible and infected individuals along with the corresponding costs associated with control $u_1(t)$ and $u_2(t)$. We consider the control variables to be bounded and Lebesgue measurable. Therefore the objective functional is expressed as follows:

$$J(u_1(t), u_2(t)) = \int_0^T \left[A\mathscr{S}_a(t) + B\mathscr{I}_a(t) + \frac{1}{2}Cu_1^2(t) + \frac{1}{2}Du_2^2(t) \right] dt \tag{52}$$

Based on the proposed model(5). As part of the objective functional, A, B denote the constants representing the weight of the susceptible and infected populations, where C and D correspond to the weight parameters linked to the control measures. More precisely C represent cost weight for treatment and D for vaccination. The terms $\frac{1}{2}Cu_1^2(t)$, $\frac{1}{2}Du_2^2(t)$ it shows cost of disease intervention. The expenses associated with control strategies $u_1(t)$ and $u_2(t)$ aries from vaccinating the susceptible cattle and treating the infected cattle respectively. The objective is to reduce the number of susceptible and infected cattle while increasing the vaccinated and recovered cattle population by applying two dynamically changing control variables $u_i(t),\ i = 1, 2$. The control function is identified such that

$$J(u_1^*, u_2^*) = minJ(u_1, u_2), u_1, u_2 \in U,$$

subjected to the suggested model (51) where the control set is expressed as,

$$U = \{(u_1, u_2) | u_i(t) \textit{ are Lebesguse measurable on } [0,1], 1 \geq u_i(t) \geq 0, i = 1, 2\}$$

Before continuing we need to confirm the existence of appropriate control measures.

5.1. Existence of Solution

We show in this paragraph that there is a solution to the control problem (5) exist. The system (5) admits a positive and bounded solution for the bounded Lebesgue measurable control functions and nonnegative beginning conditions. We look at the following finding to demonstrate the existence of the proposed model (51).

Theorem 5. *If model (5) holds then there exist a set of control measures* $u^* = (u_1^*, u_2^*) \in U$*, such that* $J(u_1, u_2) = minJ(u_1, u_2)$.

Proof. It is clear that the control measure $u_i(t)$ for $i = 1, 2$ and the state variables $(\mathscr{S}_a, \mathscr{I}_a, \mathscr{V}_a, \mathscr{R}_a, \mathscr{S}_v, \mathscr{I}_v, \mathscr{E})$ are nonnegative, U is closed and convex. System(5) is bounded and hence compact. Further, the integrand $A\mathscr{S}_a(t) + B\mathscr{I}_a(t) + \frac{1}{2}Cu_1^2(t) + \frac{1}{2}Du_2^2(t)$ the proof is finished since in model (51)is convex on U.

5.2. Conditions for Optimal Control Variables

For the optimal solution of model (51) we introduce the Lagrangian and Hamiltonian optimal problem. Lagrangian is given by

$$L(\mathscr{S}_a, \mathscr{I}_a, u_1, u_2) = A\mathscr{S}_a(t) + B\mathscr{I}_a(t) + \frac{1}{2}(Cu_1^2(t) + Du_2^2(t)) \tag{53}$$

For the Lagrangian's smallest value, define Hamiltonian H for model (5) as

$$\mathscr{H}(x, u, \lambda) = \mathscr{L}(x, u) + \lambda.\mathscr{F}(x, u), \tag{54}$$

where

$$x = (\mathscr{S}_a, \mathscr{I}_a), u = (u_1, u_2), \lambda = (\lambda_1, \lambda_2, ..., \lambda_7), \tag{55}$$

$\mathscr{F}_1(x, u) = \lambda_1\left((1-k)M_1 - \beta_a\mathscr{S}_a\mathscr{I}_v - \beta_b\mathscr{S}_a\mathscr{E} - \beta_c\mathscr{S}_a\mathscr{I}_a - (u_1(t) + \mu)\mathscr{S}_a - v_1\mathscr{S}_a + v_2\mathscr{V}_a\right)$
$\mathscr{F}_2(x, u) = \lambda_2\left(\beta_a\mathscr{S}_a\mathscr{I}_v + \beta_b\mathscr{S}_a\mathscr{E} + \beta_c\mathscr{S}_a\mathscr{I}_a - (\delta + \mu)\mathscr{I}_a - (v_2 + u_2(t))\mathscr{I}_a\right)$
$\mathscr{F}_3(x, u) = \lambda_3\left(kM_1 + v_1\mathscr{S}_a - v_2\mathscr{V}_a - \mu\mathscr{V}_a + u_1(t)\mathscr{S}_a\right)$
$\mathscr{F}_4(x, u) = \lambda_4\left(\delta\mathscr{I}_a + u_2(t)\mathscr{I}_a - \mu\mathscr{R}_a\right)$
$\mathscr{F}_5(x, u) = \lambda_5\left(M_2 - \frac{\beta_4\mathscr{S}_v\mathscr{I}_a}{N_a} - \mu_v\mathscr{S}_v\right)$
$\mathscr{F}_6(x, u) = \lambda_6\left(\frac{\beta_4\mathscr{S}_v\mathscr{I}_a}{N_a} - \mu_v\mathscr{I}_v\right)$
$\mathscr{F}_7(x, u) = \lambda_7\left(\phi\mathscr{I}_a - \omega\mathscr{E}\right)$
and $\mathscr{F}(x, u) = (\mathscr{F}_1, \mathscr{F}_2, ..., \mathscr{F}_7)(x, u)$. We decide Pontryagin's Maximum Principle in order to arrive at the best solution for the control problem that has been formulated: A non trivial function λ exists if (x_*, u_*) is an optimal solution to Eq(4.1) with u_* beginning basically limited, such that it satisfies the related Hamiltonian system.

$$\begin{cases} \frac{\partial x^*(t)}{\partial t} = \frac{\partial\mathscr{H}}{\partial\lambda}(x^*(t), u^*(t), \lambda(t)) \\ \frac{\partial\lambda^*(t)}{\partial dt} = -\frac{\partial\mathscr{H}}{\partial\lambda}(x^*(t), u^*(t), \lambda(t)) \\ 0 = \frac{\partial\mathscr{H}}{\partial\lambda}(x^*(t), u^*(t), \lambda(t)) \end{cases} \tag{56}$$

the maximality condition

$$\mathscr{H}(x^*(t), u^*(t), \lambda(t)) = max_{u_1,u_2\in[0,1]}\mathscr{H}(x^*(t), u_1, u_2, \lambda(t)) \tag{57}$$

and the transverality condition

$$\lambda(t_f) = 0 \tag{58}$$

hold.

Theorem 6. *For the optimal control problem (5) consider $\mathscr{S}_a^*, \mathscr{I}_a^*, \mathscr{V}_a^*, \mathscr{R}_a^*, \mathscr{S}_v^*, \mathscr{I}_v^*$ and $\mathscr{E}^*$ be the optimal state solutions for the bounded optimal controls variables (u_1^*, u_2^*). Then there exist adjoint variables $\lambda_i(t)$ $i = 1, 2, ..., 6$, satisfying*

$$\begin{cases} \frac{d\lambda_1}{dt} = & -A + \lambda_1\left(\beta_a\mathscr{I}_v + \beta_b\mathscr{E} + \beta_c\mathscr{I}_a + u_1(t) + \mu - v_1\right) - \lambda_2\left(\beta_a\mathscr{I}_v + \beta_b\mathscr{E} + \beta_c\mathscr{I}_a\right) \\ & -\lambda_3\left(v_1 + u_1(t)\right) \\ \frac{d\lambda_2}{dt} = & -B + \lambda_1\beta_c\mathscr{S}_a - \lambda_2\beta_c\mathscr{S}_a + \lambda_2\left(\delta + \mu + u_2(t)\right) \\ & -\lambda_4\left(\delta + u_2(t)\right) + \lambda_5\left(\frac{\beta_4\mathscr{S}_v}{N_a}\right) - \lambda_6\left(\frac{\beta_4\mathscr{S}_v}{N_a}\right) - \lambda_7\phi \\ \frac{d\lambda_3}{dt} = & \lambda_1 v_2 + \lambda_3\mu - \lambda_3 v_2 \\ \frac{d\lambda_4}{dt} = & \lambda_4\mu \\ \frac{d\lambda_5}{dt} = & \lambda_5\left(\frac{\beta_4\mathscr{I}_a}{N_a} + \mu_v\right) - \lambda_6\left(\frac{\beta_4\mathscr{I}_a}{N_a}\right) \\ \frac{d\lambda_6}{dt} = & \lambda_1\left(\beta_a\mathscr{S}_a\right) - \lambda_2\left(\beta_a\mathscr{S}_a\right) + \lambda_6\mu_v \\ \frac{d\lambda_7}{dt} = & \lambda_1\beta_b\mathscr{S}_a - \lambda_2\beta_b\mathscr{S}_a + \lambda_7\omega. \end{cases} \tag{59}$$

The conditions of transversality are

$$\lambda_i(t_f) = 0 for i = 1, 2, ..., 7. \tag{60}$$

The optimal control variable $u_1 and u_2$ are given by

$$\begin{aligned} u_1^*(t) &= max\left\{min\left\{\frac{(\lambda_1 - \lambda_3)\mathscr{S}_a}{C}, 1\right\}, 0\right\} \\ u_2^*(t) &= max\left\{min\left\{\frac{(\lambda_2 - \lambda_4)\mathscr{I}_a}{D}, 1\right\}, 0\right\}. \end{aligned}$$

Proof. Proof of the theorem is obvious.

6. Discussion of Optimal Control Simulation

These plots illustrates the impact of implementing optimal control strategies namely vaccination in plot(a) and treatment in plot(b) on the dynamics of infected cattle over a 20 day period. In the absence of control measures (red dashed line) the plot(D) of infected population rises rapidly and remains relatively high indicating a sustained transmission of the disease. However, when optimal control is applied(green solid line) a noticeable

difference is observed. The number of infected cattle initially increases but reaches a much lower peak and the declines sharply over time. This demonstrates the effectiveness of the control strategies in curbing the spread of the disease. In the plot (E) of vaccination helps by reducing the number of susceptible cattle in the plot (c) while treatment facilitates quicker in plot (f) of recovery of infected individuals. The plot (g) of susceptible insects with out control it depress quickly and with control also decrees but slowly as compered to without control. In without control the plot (h) of infected insects increase quickly and with control increase but slowly as compered to without control. In the plot (i) is contaminated environment without control it increase highly and quickly and with control it increase but slowly as compered to without control. The implementation of both control measures reduces the infection burden and shortens the duration of outbreak highlighting their crucial role in disease management.

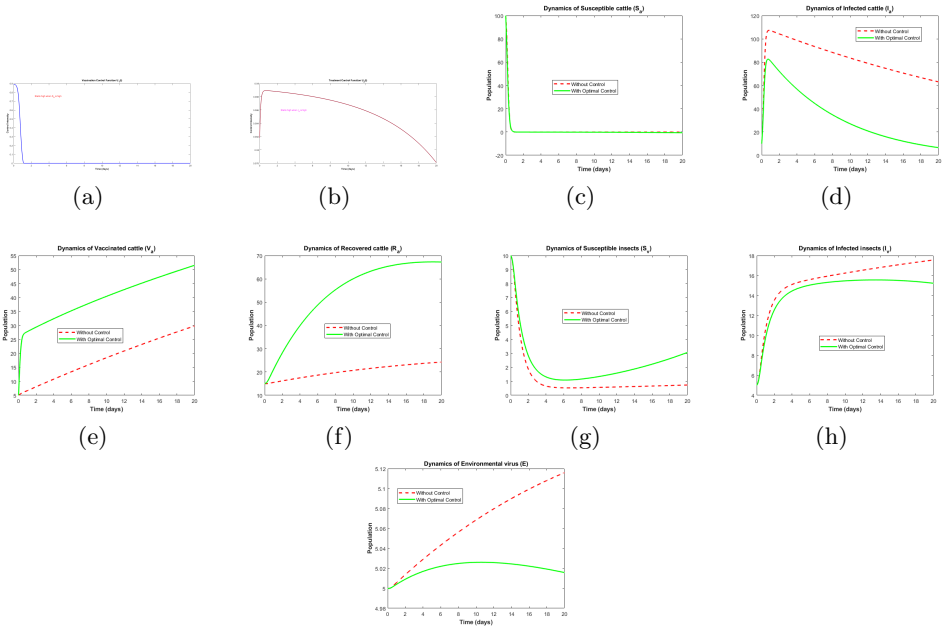

(a) (b) (c) (d)

(e) (f) (g) (h)

(i)

Figure 5: Optimal control analysis of the considered model.

7. Neural Networking of the LSD Model

7.1. ANN Training and Error Levenberg-Marquardt Algorithm-Based Error Analysis

In this work Artificial Neural Networks(ANNs) are trained using the Levenberg-Marquardit(LM) back propagation algorithm to approximate the solution to the time delay LSD epidemic model. Further a detailed discussion on how to train model for error analysis test and validate data for explanation and performance criteria of the model:

7.2. Data Set Splitting

The data set can be split in to the following three sub-categories for the optimal control of the model:

- **Training set:** Training set is used in NN for weight and biases.
- **Validation set:** Validation set is used to avoid overlapping and checking the performance. During the training, if the error is high while the training error is low, then the training will be stopped.
- **Testing set:** To handle the unseen data after training is the main theme of the testing set.

$$MSE = \frac{1}{n}\sum_{i=1}^{n}\left(y_i - p(\theta)\right)^2.$$

The mean square error(MSE) is employed as the performance metric for all subsets and is define as: where y_i is the target output from the Euler solution, $P(\theta)$ is the ANN predicated output and θ denotes the network parameters.

7.3. Levenberg-Marquardt Back-Propagation Algorithm

Levenberg-Marquard(LM) algorithm will be used for the ANNs to resolve nonlinear least squares problems due to its fast convergence and efficacy. The expression of the sum of squared errors(SSE) is given below and show the error function that needs to be minimized:

$$E(\theta) = \frac{1}{2}\sum_{i=1}^{n}\left(y_i - p(\theta)\right)^2.$$

The Levenberg-Marquardt(LM) method to utilizes the following iterative update rule to refine the parameters θ (weights and biases):

$$\theta_{new} = \theta_{old} - \left(J^T J + \lambda I\right)^{-1} J^T e,$$

where the Jacobian matrix J represents the partial derivatives of the errors with respect to the network parameters. $e = y - P(\theta)$ defines the error vector I stands for the identity matrix and the damping factor λ is adaptively changed during training to regulate the step size. This approach combines the gradient descent and Gauss-Newton techniques dynamically modifying the update rule in response to the ANN's performance on the validation set.

7.4. Error Histogram

The distribution of errors throughout the training validation and testing data sets is shown using error histograms. Each data point error is calculated as follows:

$$e(t) = y(t) - P(\theta, t),$$

where $P(\theta, t)$ is the ANN-predicated value at time t and $y(t)$ is the reference value from the Euler solution. The frequency of these errors is shown by the error histogram, where most of them are optimally clustered around zero. This provides insight into the accuracy of the model as well as the characteristics of its residual errors.

7.5. Regression analysis

Regression analysis quantifies the correlation between the ANN predictions and the target outputs from the Euler solution is employed to evaluate the ANN's performance.

$$R = \frac{\sum_{i=1}^{n}(y_i - \bar{y})\left(P(\theta) - \bar{P}\right)}{\sqrt{\sum_{i=1}^{n}(y_i - \bar{y})^2}\sqrt{\sum_{i=1}^{n}\left(P(\theta) - \bar{P}\right)^2}}$$

where y_i denotes the target output represent the ANN-predicted output and $\bar{y}$ and $P(\theta)$ are the mean values of y and $P(\theta)$, respectively.

7.6. Performance Plots and Error Analysis

The MSE is displayed across epochs in a performance plot emphasizing the ANN's convergence behavior . For every compartment the temporal development of the absolute error between the ANN outputs and the ODE solution is assessed in addition to performance measures. Each compartment's error at each time step is computed as follows:

$$e(t) = |y(t) - P(\theta, t)|$$

$e(t)$ denotes the difference among the ANN-predicted value over time and target solution.

8. Proposed Methodology: ANN-LM Approach

The Artificial Neural Network with Levenberg-Marquardt (ANN-LMB) method is employed to approximate the solution of the LSD transmission model, which is formulated using the nonlinear SIVR framework. The ANN-LMB algorithm is formulated based on the nonlinear dynamics of the models as the basis and implemented in two main stages. Using a stochastic training approach, the method integrates the structure to maximize performance across multiple network layers. The neural fitting (nf) tool in MATLAB was used for the implementation. The data set was divided into three subsets: testing (15%), validation (15%) and training (70%). The optimal network architecture comprises 10 neurons in the hidden layer with input hidden and output layers as shown in the figure. Optimization results are achieved via the ANN-LMB approach are present in figure offer important new information about the dynamics of the LSD outbreak.

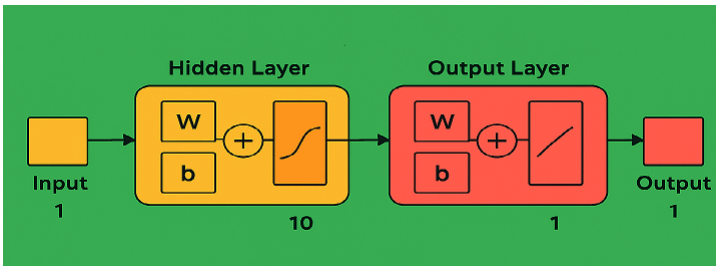

Figure 6: Structure of Deep Neural Network

Parameters	Descriptions	Parameters	Descriptions
Training data	70%	Validation data	15%
Testing data	15%	Hidden neurons	10
Maximum epochs	1000	Minimum gradient	1×10^{-7}
Data set Generation	Numerical solution of SIVR ODE (Euler)	Input/Output Neurons	1

Table 4: Parameter values used in the computation

8.1. Artificial Neuron Structure

Fig. 8 shows the basic architecture of an artificial neuron, which was first conceptualized by Mc Culloch and Pitts [23]. Based on the activation function a neuron interprets input signals and produces an output. The neuron's activity can be threshold changing the equation to:

$$y = f\left(\sum_{i=1}^{n} w_i x_i - \theta\right),$$

Here θ denotes the threshold f represents the activation function, w_i and x_i corresponding to the i^{th} weight and input, respectively. A bias term b can be used in place of the threshold, changing the equation to:

$$y = f\left(\sum_{i=1}^{n} w_i x_i + b\right), \tag{61}$$

Both linear and non-linear activation functions can be used. Because they allow for, nonlinear activation functions like the tangent sigmoid function $(f(k) = tanh(k))$ are preferred for complex tasks, as they enable nonlinear transmission of the input data. The fundamental architecture of an artificial neuron is shown in Fig **??**.

8.2. Multi-layer ANN Structure

Through collective processing, a multi-layer artificial neural network (ANN) made up interconnected neurons arranged into input hidden and output layers makes it possible to compute complex calculations. In Fig **??**, the architecture is illustrated.Describes a multi-layer artificial neural network (ANN), which offers more computing power than single-layer networks **??**.

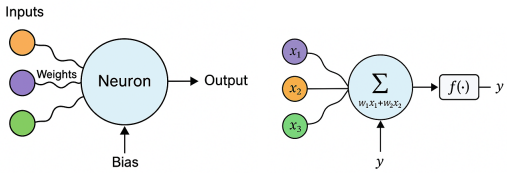

(a) Numerical Plot of S us-(b) Absolute Error of S ing DNN

(c) Train Data of S

Figure 7: Plots of Results for Susceptible (S) Node Using DNN

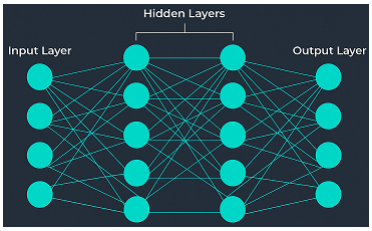

Figure 8: Structure of Deep Neural Network

9. Neural Network Simulation and Discussion

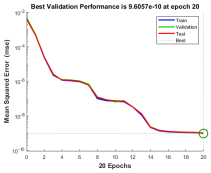

(a)

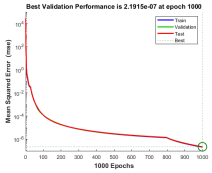

(b)

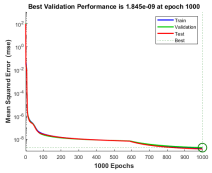

(c)

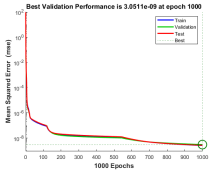

(d)

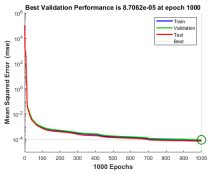

(e)

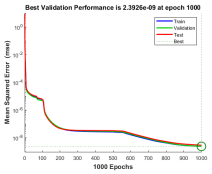

(f)

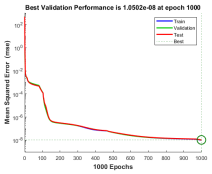

(g)

Figure 9: Means square errors plots for all classes

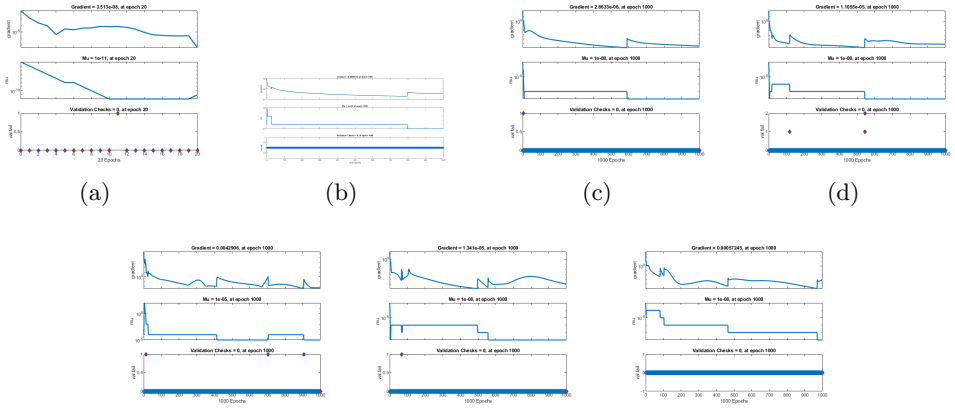

(a) (b) (c) (d)

(e) (f) (g)

Figure 10: Training performance curves demonstrating stable convergence and good generalization.

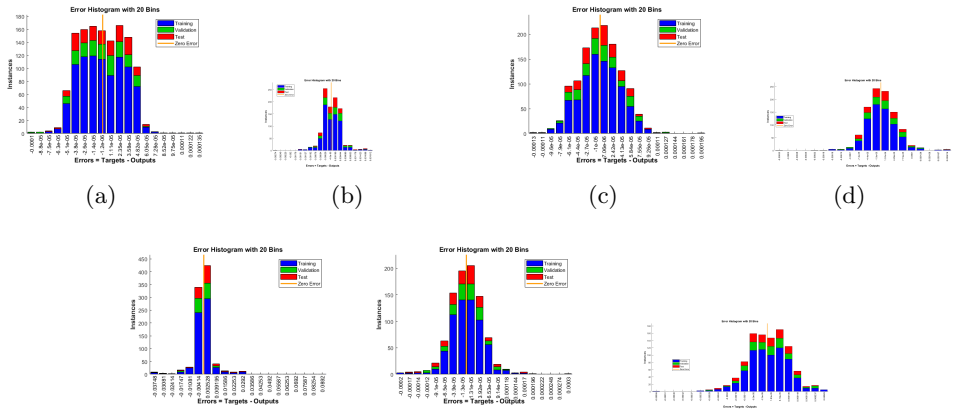

(a) (b) (c) (d)

(e) (f) (g)

Figure 11: Errors histogram plots for all classes.

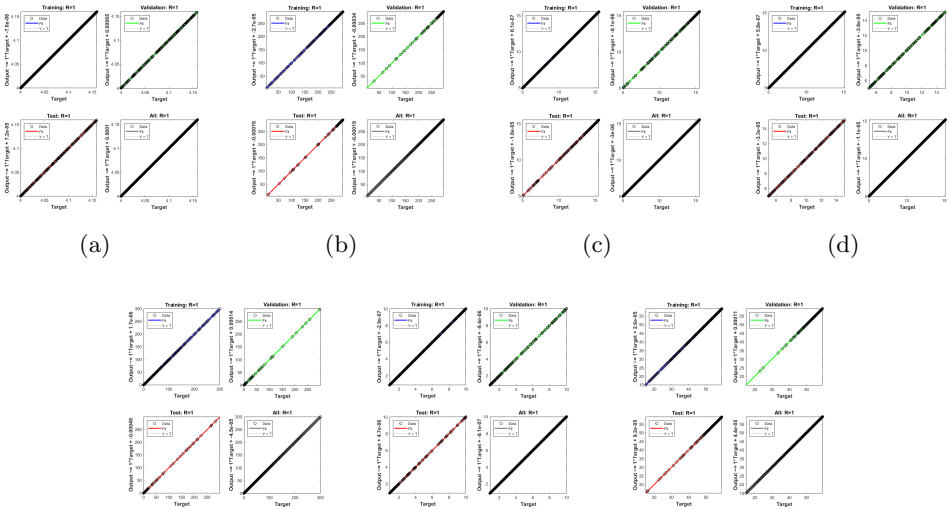

(a) (b) (c) (d)

(e) (f) (g)

Figure 12: Representation of the regression line for all classes of the considered system.

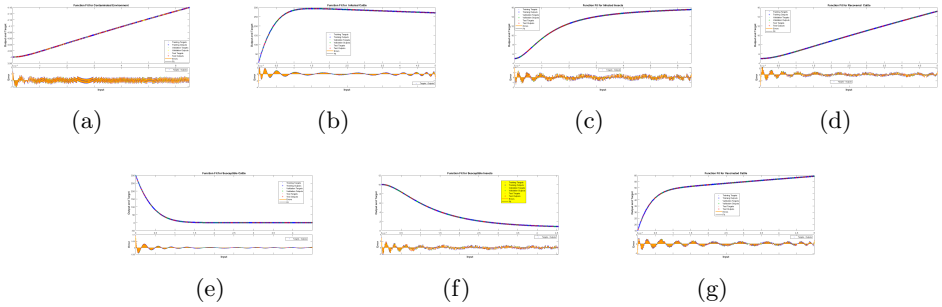

(a) (b) (c) (d)

(e) (f) (g)

Figure 13: The best fit of the training and testing data along with errors for all classes of the considered system.

In this study an artificial neural network(ANN) was employed to approximate the solution of the proposed LSD model. Illustrates the training performance of the neural network using 10,000 epochs focusing on three key metrics: Mean Squared Error(MSE) error histogram and the comparison between target and output values. The MSE plot shows a sharp decrease in error during the initial epochs eventually converging to a very small value. This behavior indicates that the neural network successfully learned the underlying patterns in the training data generated from the numerical solution of the model. The smooth convergence with minimal fluctuations further suggests that the network avoided over fitting and generalizes well within the training domain. The error histogram displays the distribution of network prediction errors. Most of the errors are clustered tightly around zero with a symmetrical and narrow shape. This reinforces the accuracy of the

Compartment	Epoch to Converge	Final (MSE)	R-value	Error Range	Fit Quality
S_a	≈ 6	1.5×10^{-15}	1.000	$-5.2e^{-8} \rightarrow +4.8e^{-8}$	Perfect
I_a	≈ 8	2.1×10^{-15}	1.000	$-6.1e^{-8} \rightarrow +5.9e^{-8}$	Perfect
V_a	≈ 5	1.1×10^{-15}	1.000	$-4.9e^{-8} \rightarrow +4.5e^{-8}$	Perfect
R_a	≈ 6	1.3×10^{-15}	1.000	$-5.0e^{-8} \rightarrow +4.8e^{-8}$	Perfect
S_v	≈ 4	1.1×10^{-15}	1.000	$-3.0e^{-8} \rightarrow +4.6e^{-8}$	Perfect
I_v	≈ 7	1.2×10^{-15}	1.000	$-2.0e^{-8} \rightarrow +4.7e^{-8}$	Perfect
E	≈ 4	1.6×10^{-15}	1.000	$-5.0e^{-8} \rightarrow +4.6e^{-8}$	Perfect

Table 5: Combine Observation Table

network and confirms that predictions closely match the target outputs. The absence of significant outliers in the histogram indicates stable learning and a well-calibrated model. The comparison plot between the network outputs and target values shows near-perfect alignment along the diagonal line $y = x$. This visual cue confirms that the ANN accurately approximates the model dynamics across the range of input values. The close correspondence validates the neural networks ability to replicate the system behavior generated from the ODE-based model. The neural network serves as an effective surrogate model providing fast approximations of the LSD dynamics without solving the differential equations repeatedly. This capability is particularly useful in control optimization and real-time forecasting applications. The strong performance across all metrics demonstrates the reliability of ANN as a tool for solving complex nonlinear systems in epidemiological modeling.

Artificial neural networks(ANNs) are powerful tools for modeling complex systems but they have limitations. Their black box nature makes interpretation difficult they require large amounts of high quality data and over fitting can reduce performance on new data. Designing the network architecture is often time consuming and training can be computationally expansive. Despite these challenges ANNs remain effective for many practical applications when carefully implemented.

10. Conclusion

In this research, we formulate a mathematical model of LSD to consider all the potential compartments through which the disease may spread in the population. We have investigated the fundamental results of the model to determine its equilibrium points (DFEP and EEP). In this model we calculate sensitivity analysis as well as stability analysis of local and global stability behaviours assuming that the basic reproductive number is less than one. We have already explored the existence, uniqueness, boundedness, and feasibility of the model's solutions. We have already added a new vaccination class to the model for control of the spread of the disease. We solve the model numerically by Euler's method, and we also present the results graphically using MATLAB . In these consequences we proved that a solution to the LSD model exists under the given initial conditions and system and system assumptions. The solution to the model is unique meaning no two different solu-

tion paths exist for the same initial conditions. Here we also prove that all state variables in the model remain finite and biologically meaningful over time. We examined the local and global stability of equilibrium points to understand the long-term behaviour of the disease. We identified the parameters that most influence disease dynamics by changes that affect the system's output. This research we have also develops an optimal control strategy for LSD model (1) used two time dependent (vaccination and treatment) as control variables in the LSD model demonstrating significant potential in reducing infection levels and controlling LSD outbreaks. Our results show that optimal application of both strategies not only lowers the number of infected cattle over time but also balances the economic costs of control. In the modeling system we just focused on the approximate solutions. An Artificial Neural Network(ANN) is also employed for approximate solutions and analyze system dynamics. In lastly on the bases of these both approach we achieved effective strategies and accurate predictions for managing this complex processes.

Acknowledgements

The authors extend their appreciation to Prince Sattam bin Abdulaziz University for funding this research work through the project number
(PSAU/2025/03/34359).

Declarations

Conflict of interest: The authors have no relevant financial or non-financial interests to disclose.
Funding information: The authors extend their appreciation to Prince Sattam bin Abdulaziz University for funding this research work through the project number
(PSAU/2025/03/34359).
Availability of Data and Material: The data regarding this manuscript is available within the manuscript.

References

[1] S Babiuk, T R Bowden, D B Boyle, D B Wallace, and R P Kitching. Capripox viruses: an emerging worldwide threat to sheep, goats and cattle. *Transboundary and Emerging Diseases*, 55:263–272, 2008.

[2] J A W Coetzer. Lumpy skin disease. infectious diseases of livestock. *Oxford University Press Southern Africa*, pages 1268–1276, 2004.

[3] S Babiuk, T R Bowden, G Parkyn, B Dalman, L Manning, J Neufeld, J E Hyatt, J Copps, and D B Boyle. Quantification of lumpy skin disease virus following experimental infection in cattle. *Transboundary and Emerging Diseases*, 55:299–307, 2008.

[4] K E Weiss. Lumpy skin disease. *Virology Monographs*, 3:111–131, 1968.

[5] F G Davies. Lumpy skin disease, an african capripox virus disease of cattle. *British Veterinary Journal*, 147:489–503, 1991.
[6] C M Chihota, L F Rennie, R P Kitching, and P S Mellor. Mechanical transmission of lumpy skin disease virus by aedes aegypti (diptera: Culicidae). *Epidemiology and Infection*, 126:317–321, 2001.
[7] C M Chihota, L F Rennie, R P Kitching, and P S Mellor. Attempted mechanical transmission of lumpy skin disease virus by biting insects. *Medical and Veterinary Entomology*, 17:294–300, 2003.
[8] I Yeruham, O Nair, Y Braverman, M Davidson, H Grinstein, M Haymovitch, and O Zamir. Spread of lumpy skin disease in israeli dairy herds. *Veterinary Record*, 137:91–93, 1995.
[9] V M Carn and R P Kitching. An investigation of possible routes of transmission of lumpy skin disease virus (neethling). *Epidemiology and Infection*, 114:219–226, 1995.
[10] FAO. Introduction and spread of lumpy skin disease in south, east and southeast asia. *FAO Report*, 2020.
[11] V M Carn. Control of capripox virus infections. *Vaccine*, 11:1275–1279, 1993.
[12] J Brenner, M Bellaiche, E Gross, D Elad, Z Oved, M Haimovitz, A Wasserman, O Friedgut, Y Stram, V Bumbarov, and H Yadin. Appearance of skin lesions in cattle populations vaccinated against lumpy skin disease: statutory challenge. *Vaccine*, 27:1500–1503, 2009.
[13] A M Khan and A Abdon. Modeling the dynamics of novel coronavirus (2019-ncov) with fractional derivative. *Alexandria Engineering Journal*, 59:2379–2389, 2020.
[14] S Ullah and A M Khan. Modeling the impact of non-pharmaceutical interventions on the dynamics of novel coronavirus with optimal control analysis. *Chaos, Solitons and Fractals*, 139:110075, 2020.
[15] Z Li et al. Distributed tracking control for linear multiagent systems with a leader of bounded unknown input. *IEEE Transactions on Automatic Control*, 58:518–523, 2012.
[16] H N Shah, A H Suthar, and E N Jayswal. Control strategies to curtail transmission of covid-19. *International Journal of Mathematics and Mathematical Sciences*, pages 1–12, 2020.
[17] E R Kopp. Pontryagin maximum principle. *Mathematics in Science and Engineering*, 5:255–279, 1962.
[18] A Ballesteros, A Blasco, and I Gutierrez-Sagredo. Hamiltonian structure of compartmental epidemiological models. *Physica D: Nonlinear Phenomena*, 413:132656, 2020.
[19] A A Lashari and G Zaman. Optimal control of a vector borne disease with horizontal transmission. *Nonlinear Analysis: Real World Applications*, 13:203–212, 2012.
[20] K Guedri, R Zarin, M Oreijah, S K Alharbi, and H A E W Khalifa. Artificial neural network driven modeling of ebola transmission dynamics with delays and disability outcomes. *Applied Mathematical Modelling*, pages 108350–115, 2025.
[21] W F Alfwzan, M H D Assi, F M Allehiany, M A Khan, M Y Alashrani, and E M Tageldin. A novel mathematical study to understand the lumpy skin disease (lsd)

using modified parameterized approach. *Results in Physics*, 51:106626, 2023.

[22] A Padder, L Almutairi, S Qureshi, A Soomro, A Aroz, and E Hincal. Dynamical analysis of generalized tumor model with caputo fractional order derivative. *Fractal and Fractional*, 7:4643–258, 2023.

[23] H Wang, M Xiao, B Tao, F Xu, Z Wang, C Huang, and J Qiu. Improving dynamics of integer order small world network models under fractional order pd control. *Science China Information Sciences*, 63:112206, 2020.

[24] C Xu, M Liao, M Farman, and A Shehzad. Hydrogenolysis of glycerol by heterogeneous catalysis: a fractional order kinetic model with analysis. *Mathematical Communications in Mathematical and Computer Chemistry*, 91:467–493, 2024.

[25] K Levenberg. A method for the solution of certain nonlinear problems in least squares. *Quarterly of Applied Mathematics*, pages 10666–115, 1944.

[26] Mati ur Rahman, Salah Boulaaras, Saira Tabassum, and Dumitru Baleanu. A deep neural network analysis of fractional omicron mathematical model with vaccination and booster dose. *Alexandria Engineering Journal*, 118:435–448, 2025.